JOURNAL OF GEOPHYSICAL RESEARCH, VOL. 113, F01S10, doi:10.1029/2006JF000653, 2008

Terrigenous organic matter in sediments from the Fly River delta-clinoform system (Papua New Guinea)

Miguel A. Goni,[1] Natalie Monacci,[2] Rachel Gisewhite,[3] John Crockett,[4] Charles Nittrouer,[4] Andrea Ogston,[4] Simone R. Alin,[4] and Rolf Aalto[5]

Received 1 August 2006; revised 30 January 2007; accepted 22 March 2007; published 2 February 2008.

[1] Although an inordinate fraction of the global sediment flux to the ocean occurs in tropical mountainous river margins, little is known regarding the sources and fate of organic matter in these systems. To address these knowledge gaps, the distribution and composition of organic matter in sediments from the Fly River delta-clinoform were examined in the context of the source-to-sink study of the Papuan Continuum. The significant contrasts in the texture of seabed sediments measured across the study area coincided with stark contrasts in concentration and composition of the sedimentary organic matter. Coarser sediments displayed significantly lower organic carbon and nitrogen contents, more enriched stable carbon and nitrogen compositions, lower lignin product yields, and distinctly different lignin and nonlignin product compositions than their fine-textured counterparts. Compositional differences were also measured between high- and low-density fractions of selected sediment samples. Subsurface sediments showed marked compositional variations that were predominantly associated with changes in the texture of the deposits. Most sediments were characterized by moderate carbon loadings (0.5–1.0 mg C m^{-2}), although several samples from the outer topset region, an area of sediment bypass, were characterized by lower carbon loadings indicative of enhanced carbon losses. Overall, the organic matter in both surface and subsurface sediments appeared to have predominantly a terrigenous origin, with no evidence for dilution and/or replacement by marine carbon. The measured compositions were consistent with contributions from modern vascular plant detritus, aged soil organic matter, and very old or fossil organic matter devoid of recognizable biochemicals.

Citation: Goni, M. A., N. Monacci, R. Gisewhite, J. Crockett, C. Nittrouer, A. Ogston, S. R. Alin, and R. Aalto (2008), Terrigenous organic matter in sediments from the Fly River delta-clinoform system (Papua New Guinea), *J. Geophys. Res.*, *113*, F01S10, doi:10.1029/2006JF000653.

1. Introduction

[2] Clinoforms are sigmoidal-shaped sedimentary deposits that dominate the stratigraphy of continental margins [e.g., *Vail et al.*, 1977; *Christie-Blick and Driscoll*, 1995]. Many river-dominated shelves display large subaqueous delta-clinoform systems that result from the accumulation of fluvial sediments [e.g., *Alexander et al.*, 1991; *Harris et al.*, 1993; *Kuehl et al.*, 1986, 1989; *Nittrouer et al.*, 1986; *Walsh et al.*, 2004]. Elevated inputs of recalcitrant organic matter (OM) and high mass accumulation rates make these systems some of the most significant sites of carbon burial in the present-day ocean [e.g., *Berner*, 1982; *Hedges and Keil*, 1995]. Because of the high precipitation and steep terrain, mountainous wet-tropical margins are especially important for the global sediment supply to the ocean [e.g., *Milliman and Syvitski*, 1992; *Nittrouer and Kuehl*, 1995]. Less is known about the role these margins play on the global carbon budget. However, because the transport and fate of particulate OM in river-dominated continental margins are controlled to a large degree by dispersal and deposition of sediments [e.g., *Alongi et al.*, 1992; *Gordon et al.*, 2001; *Leithold and Blair*, 2001; *Blair et al.*, 2004; *Goni et al.*, 2005a], it is likely that tropical mountainous rivers are globally significant in terms of the delivery and sequestration of land-derived OM in the ocean.

[3] The delivery, redistribution and accumulation of sediments and associated materials in river-dominated margins are affected by several physical processes, such as river discharge, tides, and waves, all of which vary significantly

[1]College of Oceanic and Atmospheric Sciences, Oregon State University, Corvallis, Oregon, USA.
[2]School of Fisheries and Ocean Sciences, University of Alaska Fairbanks, Fairbanks, Alaska, USA.
[3]Department of Marine Sciences, University of Georgia, Athens, Georgia, USA.
[4]School of Oceanography, University of Washington, Seattle, Washington, USA.
[5]Department of Earth and Space Sciences, University of Washington, Seattle, Washington, USA.

0148-0227/08/2006JF000653$09.00

over different spatial and temporal scales. Partially as a result of this variability, a broad range of depositional environments is typically encountered within subaqueous deltas and clinoforms [e.g., *Kuehl et al.*, 1986; *Aller*, 2001; *Aller et al.*, 2004]. Such heterogeneity in the physical and geological characteristics of nearshore environments fundamentally impacts biological and geochemical processes. Thus, for example, within these systems it is possible to encounter areas of high sediment accumulation and OM preservation adjacent to regions of intense physical mixing, where effective degradation of OM can occur [e.g., *Aller et al.*, 2004; *Gordon and Goni*, 2003; *Goni et al.*, 2005b]. In order to quantitatively understand the fate of both terrigenous and marine OM in delta-clinoform systems, it is critical to account for the variable and dynamic nature of their sedimentary environments.

[4] The source-to-sink study of the Papuan Continuum provides a unique opportunity to investigate the sources and fates of different types of OM in a tropical delta-clinoform system within the broader context of the processes regulating the input, routing and accumulation of sediment and associated materials. The overarching goal of this research is to determine the connections between the biogeochemistry of river deltaic systems and the physical and geological processes that control the dispersal of materials in these critical regions of ocean margins. With that goal in mind, we investigated the accumulation and cycling of OM in the sediments of the inshore regions of the Fly River delta-clinoform system. The specific objectives of this paper are (1) to examine the spatial distribution of OM in seabed sediments from the topset regions of the clinoform, (2) to investigate its sources using a combination of bulk and compound-specific analyses, and (3) to assess the in situ degradation and burial of OM in subsurface sediments. This work builds on previous studies of organic matter distribution [e.g., *Bird et al.*, 1995; *Robertson and Alongi*, 1995; *Alongi et al.*, 1992], which indicate terrigenous OM is a major source of the carbon present in surface sediments of the clinoform regions in the Gulf of Papua. Our investigations also incorporate insights from previous studies into the physical processes that control the transport, composition and accumulation of particles in the Gulf of Papua [e.g., *Walsh et al.*, 2004; *Goni et al.*, 2006; *Ogston et al.*, 2007; *Martin et al.*, 2007; *Crockett et al.*, 2008]. The findings from this work apply to delta-clinoform regions in general, where spatial heterogeneity and variability in physical forcings fundamentally affect the cycling of OM.

2. Background on Study Site

[5] The hydrological, oceanographic, geological and geochemical characteristics of the study area have been reviewed in previous publications [e.g., *Brunskill*, 2004; *Harris et al.*, 2004; *Walsh et al.*, 2004; *Goni et al.*, 2006, and references therein]. An overview of the most salient features of the Fly River delta-clinoform dispersal system with regards to OM cycling is provided here. The Fly River and its major tributary, the Strickland River, drain the upland regions of the Western Highlands of Papua New Guinea. Together, these rivers discharge on average 6,000 $m^3\ s^{-1}$ of water and 4 $t\ s^{-1}$ of sediment. Other sources of freshwater and sediment to the Gulf of Papua include rivers to the northeast of the Fly River, such as the Bamu, Turama and Purari rivers and those draining through the Aird River delta. Because of consistently elevated precipitation, river discharge to the coast is high and relatively constant. The major exceptions are El Niño periods, when extensive droughts can dramatically reduce river levels [*Dietrich et al.*, 1999]. Notably, a strong El Niño was active during our cruise in January 2003 and river discharge was quite low. For example, the discharge from Strickland River during this period ranged from 400–600 $m^3\ s^{-1}$, as compared with typical discharges of 3,000 to 4,000 $m^3\ s^{-1}$ [*Aalto et al.*, 2007].

[6] The geology of Papua New Guinea, which has been described by *Davies et al.* [2005] and illustrated by *Bain et al.* [1973], affects the composition of the particulate load exported by its rivers. Papua New Guinea contains three major geologic provinces: the southwest plains region (craton); the central collision zone, which forms a fold belt that makes up the highlands; and the northeastern volcanic islands. The Fly and Strickland rivers originate within the fold belt and flow across the plains to the south. The highland region is largely composed of metamorphosed Mesozoic sediments faulted against ultramaphic rocks, ophiolite, volcanic rocks and Cenozoic clastic sediments. In contrast, the southern plains comprise Mesozoic and Cenozoic sediments resting on weakly deformed Paleozoic and Precambrian cratonic basement.

[7] Abundant (up to 10 m a^{-1}) rainfall characterizes the drainage basin, which is predominantly covered by rain forests (C_3 vegetation) that range from the highlands (up to 4,500 m above sea level) to the lowland regions (0–1,500 m above sea level). A strong positive relationship exists between altitude and the stable isotopic composition of organic carbon ($\delta^{13}C_{org}$) in both the C_3 vegetation and the underlying soil OM [*Bird et al.*, 1994]. Enriched values ($\delta^{13}C_{org} > -26$ ‰) are found at altitudes above 3,000 m whereas depleted values ($\delta^{13}C_{org} < -26$ ‰) characterize locations close to sea level. Such contrasts reflect differences in the conditions (e.g., gas pressure, temperature) affecting plant growth at different altitudes [*Korner et al.*, 1988, 1991]. Besides the C_3 rain forests, grasslands are also found throughout the drainage basin. Their distribution is thought to be controlled primarily by human disturbances, predominantly burning and agriculture, which limit the growth of woody plants [*Bird et al.*, 1994, and references therein]. There is a strong relationship between altitude and the relative abundances of C_3 and C_4 grass species, with C_3 species dominating locations higher than 2,000 m above sea level whereas C_4 species become predominant in locations below this level [*Bird et al.*, 1994].

[8] The Fly River delta is tidally dominated, with maximum tidal amplitudes of 3.5–5 m and peak tidal currents of over 1 m s^{-1} [e.g., *Harris et al.*, 2004; *Wolanski et al.*, 1995, 1997]. The sediment discharge through its distributaries eventually reaches the inner shelf, where it contributes to the build up of ~100 km wide clinoform extending seaward across the northern Gulf of Papua (Figure 1) [*Walsh et al.*, 2004]. Active pathways of sediment dispersal include the Far Northern entrance, which delivers sediments to the NE region of the delta-clinoform system, as well as the

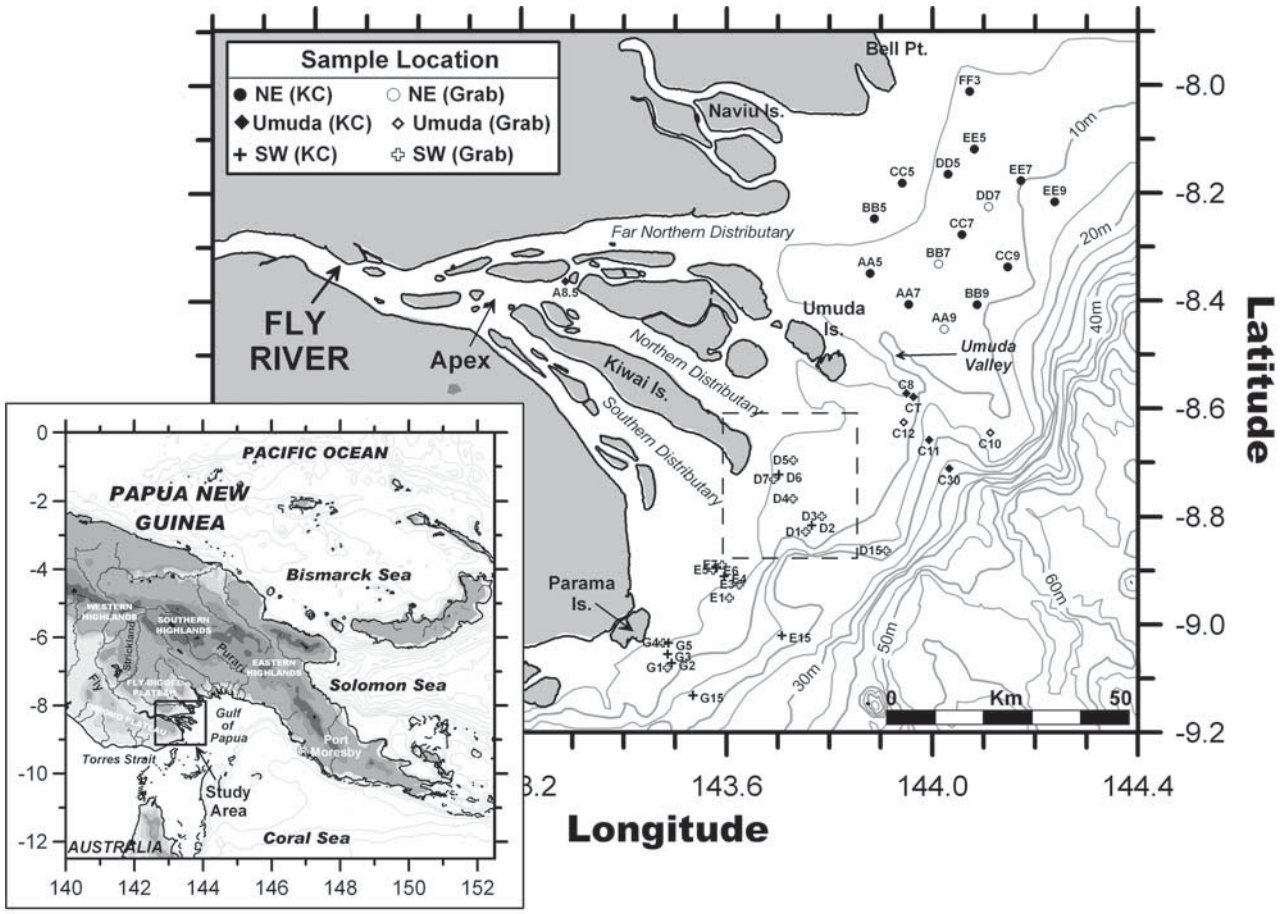

Figure 1. Map of the study area. The locations of stations from different regions of the subaqueous delta and topset region of the clinoform are indicated in the map. Open symbols are used to indicate the locations of grab samples (GB), while solid symbols indicate the locations of sites collected via kasten core (KC).

Umuda Valley (see Figure 1). Smaller uncharted channels exist offshore from the other distributaries, which connect the river with the SW region of the delta-clinoform system. Recent studies indicate that sediment accumulation rates are quite low in the SW region, suggesting that much of the sediment leaves the delta through the northern distributaries [e.g., *Crockett*, 2006; *Ogston et al.*, 2007; *Walsh et al.*, 2004].

[9] Once particulate materials leave the delta distributaries, they are further dispersed by the combined action of tides, winds and waves. The wind and wave climate of the Gulf of Papua is characterized by two seasons. During the monsoon season (December–March), winds blow southeastward off the land and, because of the short fetch, relatively calm seas (0.3 m significant wave heights) predominate [*McAlpine and Keig*, 1983; *Thom and Wright*, 1983]. During the reminder of the year (May–October), SE trade winds average 5 to 8 m s^{-1} and blow northwestward and northward, leading to much more energetic conditions (1.3 m average significant wave heights). The large-scale ocean circulation is dominated by a clockwise gyre in the northern Coral Sea, causing a predominant eastward transport along the shelf. Overall, these conditions facilitate the transport of fine sediments along and across the shelf, leading to the formation of a well-developed clinoform with characteristic topset (10–25 m of water depth), foreset (25–50 m water depth) and bottomset (50–70 m water depth) areas [e.g., *Walsh and Nittrouer*, 2003; *Walsh et al.*, 2004; *Ogston et al.*, 2007].

[10] Sediment accumulation rates based on ^{210}Pb profiles have been determined throughout the Fly River delta-clinoform system [*Harris et al.*, 1993; *Walsh et al.*, 2004; *Crockett*, 2006; *Crockett et al.*, 2008]. Accumulation rates are quite variable, ranging from negligible to >5 g cm^{-2} a^{-1}. The highest rates are measured in the NE region of the foreset (1.3 to >5 g cm^{-2} a^{-1}), with lower rates along the SW foreset region (0.5–2.0 g cm^{-2} a^{-1}). Accumulation rates are also elevated along the Umuda Valley (0.4–1.3 g cm^{-2} a^{-1}) and the inner areas of the NE topset (0.5 to 2.5 g cm^{-2} a^{-1}). Benthic macrofauna are absent from most of these deposits because of the high sediment deposition and physical mixing [e.g., *Alongi*, 1995; *Aller and Aller*, 2004]. In contrast, sediment accumulation rates are relatively low (<0.5 g cm^{-2} a^{-1}) [*Crockett et al.*, 2008] along the outer

topset of the clinoform, an area where *Martin et al.* [2008] show evidence for bioturbation in recently deposited layers.

[11] Terrigenous OM exported by the river and from the delta islands is the major source of carbon in the regions adjacent to the Fly River delta [*Bird et al.*, 1995; *Roberston and Alongi*, 1995; *Goni et al.*, 2006]. Production by marine algae is low in the inshore regions because of the high turbidity, but increases seaward as the particulate load settles from the surface waters [e.g., *Alongi et al.*, 1992; *Ayukai and Wolanksi*, 1997; *Davies*, 2004; *Robertson et al.*, 1993, 1998; *McKinnon et al.*, 2007]. Marine contributions to the sedimentary OM become progressively more important in the more distal locations of the gulf as the supply of land-derived clastic sediments decreases away from the clinoform region [*Bird et al.*, 1995]. Active degradation of both autochthonous and allochthonous OM by microorganisms takes place in the physically mixed, mobile muds that characterize some of the inshore regions in the gulf [e.g., *Aller and Blair*, 2004; *Aller et al.*, 2004, 2007].

3. Methods

3.1. Sample Collection

[12] Sediments from the inshore regions of the Fly River subaqueous delta and topset region of the clinoform (<20 m water depth) were collected in January 2003 aboard the Ok Tedi Company's vessel Western Venturer (Figure 1). During the cruise, in order to choose appropriate coring sites, we surveyed the bathymetry of this poorly charted region using a Fathometer prior to sediment collection. The heterogeneous bathymetry in some areas resulted in highly variable sediment compositions and textures, which fundamentally affected the compositions of the sedimentary OM. Special efforts were made to obtain representative samples from all locations, including fine as well as coarse sediments. With that goal in mind, seabed sediments were collected using either a kasten corer or a Shipek grab sampler with the latter being used at sandy sites where coring failed. Once collected, the kasten cores, which were up to 3 m in length, were subsampled on the ship at 1 or 2 cm intervals. In the case of the grab samples, the top 2 cm of sediment was subsampled. All sediment samples were stored frozen in sealed Kpak bags until they were analyzed. The sampling stations and the distribution of kasten and grab samples among the three major depositional areas identified within Fly River delta-clinoform system (northeast region, Umuda Valley, southwest region) are illustrated in Figure 1.

3.2. Analytical Details

[13] Prior to chemical analyses, sediments were oven dried (50°C) and ground. Unground splits of the samples were preserved for surface area analyses. A selected number of samples was fractionated by heavy liquid flotation using a dense solution (1.9 g cm^{-3}) of aqueous sodium polytungstate [*Bock and Mayer*, 2000]. Samples were suspended in the heavy solution and then centrifuged to separate the low- and high-density fractions. Each sample was treated this way three times to insure complete separation. The low-density fractions were recovered by filtering the solution onto precombusted glass fiber filters, whereas the high-density fractions were recovered in the bottom of the centrifuge tubes. Both fractions were rinsed with distilled water, dried and weighed prior to chemical analyses. Visual inspection of the low-density fractions showed significant amounts of recognizable plant detritus.

[14] All the methods utilized to characterize the compositions of the sediments and associated OM have been applied previously in coastal settings. Briefly, the weight percent contents of total carbon (%TC), organic carbon (%OC), inorganic carbon (%IC) and organic nitrogen (%ON) in all sediments were determined by high-temperature combustion using the approach outlined in previous studies [e.g., *Goni et al.*, 2003, 2006]. %IC contents were determined as the difference between %TC and %OC. %ON contents were determined after correcting for the presence of inorganic nitrogen within the total nitrogen measured according to *Goni et al.* [2003]. The stable carbon isotopic compositions of OC ($\delta^{13}C_{org}$) and nitrogen ($\delta^{15}N$) in sediment samples were analyzed after the removal of inorganic carbonates with 10% HCl, using high-temperature combustion coupled with isotope ratio mass spectrometry [e.g., *Goni et al.*, 2005a]. In selected samples, the radiocarbon contents of sedimentary OC ($\Delta^{14}C_{org}$) were determined using accelerator mass spectrometry according to the procedure of *Vogel et al.* [1987]. The $\Delta^{14}C_{org}$ data were used to estimate the age of the sedimentary organic matter and reported as fraction of modern carbon according to international convention [*Stuiver and Polach*, 1977]. The mineral surface areas (SA) of unground, OM-free sediments were determined according to the Brunauer, Emmett and Teller (BET) technique [e.g., *Mayer*, 1994; *Goni et al.*, 2005b]. Samples were precombusted at 300°C for 12 h to remove OM and degassed under vacuum for 1 h at 250°C prior to the five-point BET measurement.

[15] Alkaline CuO oxidations were performed to measure the yields of lignin- and nonlignin-derived products using a microwave digestion system according to *Goni and Montgomery* [2000]. Briefly, alkaline CuO oxidations were carried out with oxygen-purged 2N NaOH at 150°C for 1.5 h using a microwave digestion system. After the oxidation, recovery standards (ethyl vanillin, transcinnamic acid) were added and the solution was acidified to pH 1 with concentrated HCl. Samples were then extracted with ethyl acetate. Extracts were evaporated to dryness under a stream of N_2. The CuO reaction products were redissolved in pyridine and derivatized with bis trimethylsilyl trifluoroacetamide (BSTFA) + 1% trimethylchlorosilane (TMCS) to silylate exchangeable hydrogens prior to analysis by gas chromatography–mass spectrometry (GC-MS).

[16] The yields of individual lignin and nonlignin oxidation products were quantified by GC-MS using selective ion monitoring. The compounds were separated chromatographically in a 30 m × 250 μm DB1 (0.25 μm film thickness) capillary GC column, using an initial temperature of 100°C, a temperature ramp of 4°C min^{-1} and a final temperature of 300°C. The MS was run in electron impact mode, monitoring positive ions from a range of 50 to 650 amu. External calibration standards were determined for individual compounds using ions specific to each chemical structure. The calibrations, which were performed on a regular basis to test the response of the GC-MS, were highly linear ($r^2 > 0.99$) over the concentration ranges measured in the samples.

Table 1. Compositions of Surface Sediments From Fly River Delta[a]

Station	Type	SA, m^2/g	Percent ON, wt %	Percent OC, wt %	Percent IC, wt %	$\delta^{15}N$, ‰	$\delta^{13}C$, ‰	CuO Oxidation Product Yields, mg/100 mg OC				
								V_{COP}	S_{COP}	C_{COP}	B_{COP}	P_{COP}
River channel												
A8.5	KC	26.5	0.11 ± 0.00	1.21 ± 0.00	0.00	1.73 ± 0.24	−26.4 ± 0.08	1.63 ± 0.10	1.20 ± 0.06	0.139 ± 0.022	0.352 ± 0.032	0.428 ± 0.034
Northeast region												
AA5	KC	22.5	0.12 ± 0.01	1.20 ± 0.00	0.00	2.14 ± 0.63	−26.2 ± 0.15	1.76 ± 0.16	1.49 ± 0.13	0.139 ± 0.054	0.368 ± 0.030	0.341 ± 0.034
AA7	KC	19.7	0.12 ± 0.00	1.52 ± 0.07	0.013 ± 0.02	1.89 ± 0.18	−26.5 ± 0.09	2.89	2.38	0.177	0.386	0.439
AA9	Grab	5.9	0.02	0.25	0.017	−0.28	−23.9	0.15	0.05	0.018	0.173	0.090
BB5	KC	20.1	0.13 ± 0.01	1.58 ± 0.04	0.00	1.88 ± 0.47	−26.7 ± 0.15	3.58	2.39	0.226	0.860	0.867
BB7	Grab	15.8	0.07	0.85	0.00	1.93	−25.9	2.46	1.64	0.121	0.371	0.485
BB9	KC	17.7	0.10 ± 0.00	1.24 ± 0.07	0.006 ± 0.00	2.16 ± 1.55	−26.2 ± 0.04	2.88	2.00	0.179	0.327	0.555
CC5	KC	23.3	0.13 ± 0.00	1.51 ± 0.05	0.010 ± 0.02	2.04 ± 0.26	−26.4 ± 0.06	2.68	1.94	0.170	0.645	0.602
CC7	KC	22.9	0.12 ± 0.02	1.37 ± 0.18	0.060 ± 0.08	1.31 ± 0.15	−26.5 ± 0.09	2.82	1.81	0.164	0.351	0.607
CC9	KC	15.2	0.07 ± 0.01	0.91 ± 0.12	0.00	1.55 ± 0.83	−26.0 ± 0.31	1.59	1.24	0.081	0.290	0.337
DD5	KC	17.0	0.10 ± 0.00	1.28 ± 0.06	0.075 ± 0.16	1.67 ± 0.10	−26.5 ± 0.06	4.01 ± 0.23	2.49 ± 0.14	0.192 ± 0.026	0.403 ± 0.047	0.798 ± 0.053
DD7	Grab	6.7	0.03	0.28	0.022	1.19	−24.1 ± 0.15	0.28	0.12	0.038	0.217	0.115
EE5	KC	21.1	0.12 ± 0.01	1.40 ± 0.08	0.005 ± 0.01	1.79 ± 0.01	−26.4 ± 0.01	2.88 ± 0.08	2.00 ± 0.06	0.151 ± 0.010	0.695 ± 0.036	0.656 ± 0.046
EE7	KC	18.9	0.11 ± 0.01	1.73 ± 0.45	0.00	1.62 ± 0.04	−26.8 ± 0.31	3.56	2.99	0.213	0.770	0.800
EE9	KC	13.0	0.06 ± 0.01	1.07 ± 0.14	0.00	1.09 ± 0.24	−26.5 ± 0.13	3.44	1.87	0.136	0.310	0.588
FF3	KC	25.0	0.12 ± 0.01	1.33 ± 0.12	0.056 ± 0.14	1.85 ± 0.14	−26.4 ± 0.02	2.62 ± 0.06	1.96 ± 0.04	0.130 ± 0.018	0.443 ± 0.046	0.675 ± 0.030
Umuda Valley												
C10	Grab	<10	0.03	0.44	0.00	1.11	−24.2	0.26	0.17	0.105	0.168	0.136
C8	KC	17.0	0.08 ± 0.00	0.85 ± 0.03	0.19 ± 0.26	1.77 ± 0.23	−25.7 ± 0.11	1.16	0.85	0.118	0.302	0.319
C12	Grab	<10	0.02	0.37	0.00	n.m.	−24.2	n.m.	n.m.	n.m.	n.m.	n.m.
CT	KC	18.6	0.10 ± 0.01	1.08 ± 0.23	0.00	1.73 ± 0.38	−26.2 ± 0.20	2.14	1.54	0.132	0.336	0.507
C11	KC	26.0	0.13 ± 0.00	1.38 ± 0.06	0.00	2.06 ± 0.02	−26.0 ± 0.01	1.62	1.22	0.114	0.317	0.408
C30	KC	22.5	0.11 ± 0.00	1.25 ± 0.01	0.00	2.07 ± 0.36	−25.9 ± 0.02	1.95	1.49	0.130	0.340	0.407
Southeast region												
D1	Grab	<10	0.02 ± 0.00	0.27 ± 0.03	0.00	n.m.	−23.4 ± 0.17	0.10	0.05	0.021	0.083	0.015
D2	KC	13.5	0.07 ± 0.01	0.99 ± 0.14	0.00	1.65 ± 0.12	−26.5 ± 0.00	2.14	1.48	0.135	0.289	0.397
D3	Grab	<10	0.02	0.22	0.00	0.56	−23.8	n.m.	n.m.	n.m.	n.m.	n.m.
D4	Grab	<10	0.03	0.36	0.00	1.15	−25.0	1.12	0.61	0.155	0.257	0.201
D5	Grab	<10	0.02	0.27	0.00	1.39	−24.3	0.11	0.08	n.m.	0.155	0.026
D6	KC	10.1	0.06 ± 0.01	0.99 ± 0.23	0.00	1.44 ± 0.25	−26.4 ± 0.36	3.58	2.23	0.206	0.340	0.570
D7	Grab	<10	0.03	0.41	0.119	1.38	−23.9					
D15	Grab	19.1	0.05	0.56	0.043	−0.87	−25.2	1.27	0.87	0.172	0.304	0.326
E1	Grab	<10	0.04	0.37	0.00	1.38 ± 0.68	−24.3 ± 0.28	n.m.	n.m.	n.m.	n.m.	n.m.
E3	Grab	9.2	0.04 ± 0.00	0.43 ± 0.02	0.00	1.44 ± 0.29	−24.2 ± 0.29	0.52 ± 0.03	0.31 ± 0.03	0.167 ± 0.017	0.235 ± 0.028	0.213 ± 0.019
E4	KC	15.3	0.07 ± 0.01	0.87 ± 0.13	0.015 ± 0.11	1.70 ± 0.41	−25.6 ± 0.35	1.68	1.50	0.153	0.351	0.304
E5	Grab	n.m.	0.08	0.92	0.00	1.86	−26.1	n.m.	n.m.	n.m.	n.m.	n.m.
E6	KC	14.1	0.13 ± 0.01	2.41 ± 0.36	0.00	1.67 ± 0.02	−27.2 ± 0.13	5.39	3.54	0.249	0.380	0.807
E7	Grab	6.7	0.02	0.23	0.00	n.m.	−23.4	0.85	0.40	0.195	0.270	0.213
E15	KC	13.6	0.07 ± 0.01	1.04 ± 0.16	0.00	1.68 ± 0.00	−26.2 ± 0.20	2.38	1.57	0.118	0.296	0.406
G1	Grab	n.m.	0.08	4.67	0.282	2.95	n.m.	n.m.	n.m.	n.m.	n.m.	n.m.
G2	KC	13.9	0.09 ± 0.00	1.98 ± 0.06	0.00	2.53 ± 0.52	−25.1 ± 0.21	1.06	0.64	0.099	0.177	0.207
G3	KC	15.7	0.08 ± 0.00	1.37 ± 0.10	0.00	2.18 ± 0.03	−25.9 ± 0.21	2.01 ± .20	1.37 ± 0.13	0.106 ± 0.030	0.227 ± 0.010	0.267 ± 0.021
G4	Grab	n.m.	0.07	1.73	0.279	2.25 ± 0.40	−24.3 ± 0.08	0.99	0.64	0.083	0.121	0.155
G5	KC	25.0	0.05	0.74	0.00	0.06	−24.8	1.00	0.57	0.143	0.237	0.262
G15	KC	16.1	0.09 ± 0.00	1.61 ± 0.03	0.00	2.40 ± 0.29	−24.7 ± 0.10	1.01 ± 0.07	0.72 ± 0.07	0.093 ± 0.021	0.192 ± 0.012	0.232 ± 0.030

[17] Among the CuO oxidation products (COP) detected, we quantified lignin-derived compounds, including vanillyl (V_{COP}; vanillin, acetovanillone, vanillic acid), syringyl (S_{COP}; syringealdehyde, acetosyringone, syringic acid) and cinnmamyl (C_{COP}; *p*-coumaric acid, ferulic acid) products. All of these compounds are characteristically recovered from the alkaline oxidation of lignin, a phenolic macromolecule that is uniquely synthesized by vascular land plants (i.e., trees, grasses). Lignin-derived compounds have been used to quantitatively trace contributions from terrigenous OC sources in a variety of environments [e.g., *Hedges et al.*, 1986; *Goni and Thomas*, 2000; *Benner and Opsahl*, 2001; *Gordon and Goni*, 2004]. Typical yields of total lignin-derived COP (Λ_{COP}) from vascular plant tissues range from 5 to 20 mg per 100 mg of OC, depending on the overall lignin content. In addition to the lignin products, several nonlignin COP were quantified, including *p*-hydroxybenzenes (P_{COP}; *p*-hydroxybenzaldehyde, *p*-hydroxyacetopheone, *p*-hydroxybenzoic acid) and other benzoic acids (B_{COP}; benzoic acid, *m*-hydroxybenzoic acid, 3, 5-dihydroxybenzoic acids). These compounds have multiple biochemical precursors, such as aromatic amino acids, phenolic polymers such as tannins, and are produced by several OM sources, including algae, vascular plants, fungi and bacteria. Typical yields of these nonlignin COP from different natural OM sources range from 0.2 to 4 mg per 100 mg OC depending on the type of material analyzed [e.g., *Goni and Hedges*, 1995; *Goni and Thomas*, 2000]. These and other nonlignin COP have been used to trace OM contributions from various sources in different environments [e.g., *Goni and Hedges*, 1995; *Goni et al.*, 2000].

[18] Stable carbon isotopic analyses of individual COP were conducted by isotope ratio monitoring–gas chromatography–mass spectrometry (IRM-GC-MS) according to the technique of *Goni and Eglinton* [1996]. Briefly, splits of the CuO extracts were prepared in the same fashion as for GC-MS analyses and run on a GC interfaced with an isotope ratio MS. Once the samples were run, we used the known isotopic composition of the ethylvanillin and *t*-cinnamic acid recovery standards to calculate the isotopic composition of the trimethylsilyl carbons added by isotopic mass balance. The $\delta^{13}C$ compositions of the trimethylsilyl carbons determined for each sample were used to derive the $\delta^{13}C$ signatures of the COP. We estimated the reproducibility of the procedure by performing triplicate analyses of selected samples. In general, the precision of the measurement of a single compound was within 1.0 ‰.

[19] The variability associated with parameters derived from individual measurements was calculated using propagation of error [*Taylor*, 1997]. Standard deviations (σ_x) and standard errors (s.e. = $\sigma_x\, n^{-1/2}$, n is the number of samples) were used to summarize the variability among different sample sets. ANOVA tests were used to assess statistically significant differences. Unless specifically stated, all statistically significant differences reported are above the 95% confidence interval (*P* value of 0.05).

4. Results

4.1. Compositions of Surface Sediments

[20] The compositions of surface sediments throughout the study area are presented in Table 1. The spatial trends in bulk parameters have been discussed previously [*Goni et al.*, 2006]. In this paper we focus on the spatial heterogeneity displayed by the surface and subsurface samples, with special emphasis on the role that sediment texture plays in determining the geochemical composition of the sediments. For example, several uncharted shallow channels cross the SW region of the delta-clinoform system and the stations along transect D intersected one of these channel features (Figure 2). As can be seen from the compositions along transect D, the differences in bathymetry lead to stark contrasts in sediment compositions (Figure 2). The channel bottoms contained finer sediments with higher %OC contents and more depleted $\delta^{13}C_{org}$ values than their counterparts collected from the shallower channel sides. Most likely, the channels act as conduits for sediment transport [*Ogston et al.*, 2007] and, because of their deeper bathymetry, also allow for the deposition of fine sediments, which are winnowed away from the shallower sites by tidal and wave energy.

[21] Overall, as discussed by *Goni et al.* [2006], sediments from the NE region yielded higher values of %OC, %ON, lower %IC and more depleted $\delta^{15}N$ and $\delta^{13}C_{org}$ values than those along the Umuda Valley region and the SW region. However, close inspection of the data set shows that these spatial trends were mainly due to differences in texture of the sediment samples, as measured by mineral surface area (Table 1). Grain size analyses of selected samples showed that there is a significant ($r^2 = 0.70$), positive relationship between the texture of sediments and their mineral SA [*Goni et al.*, 2006]. The differences in the abundance of coarse sediment are related to the differential supply of fine sediments between the NE and SW regions [e.g., *Ogston et al.*, 2007] and the underlying bathymetry of the two areas [e.g., *Crockett*, 2006].

[22] In order to understand the trends in the geochemical composition of the seabed, it is useful to consider the compositions of coarse sediments (SA < 10 $m^2\ g^{-1}$) separate from those of fine-texture samples (SA > 10 $m^2\ g^{-1}$; Figure 3). We chose the <10 $m^2\ g^{-1}$ level as a cutoff because it roughly corresponds to sediments with a median diameter >12 μm [*Goni et al.*, 2006] and a percent sand content >6% based on grain size data [*Crockett*, 2006]. Irrespective of their geographic location, finer sediments collected throughout the delta-clinoform system had %OC contents (~1.2 wt %) that were much higher than those of coarser sediments (0.3–0.5 wt %). In the case of %ON, the high-SA samples from the SW region displayed lower

Notes to Table 1.

[a]Surface is 0–2 cm. Column headings: SA, mineral surface area; ON, organic nitrogen; OC, organic carbon; IC, inorganic carbon; V_{COP}, vanillyl CuO oxidation products (vanillin + acetovanillone + vanillic acid); S_{COP}, syringyl COP (syringealdehyde + acetosyringone + syringic acid); C_{COP}, cinnamyl COP (p-coumaric acid+ferulic acid); B_{COP}, benzoic acid COP (benzoic acid + m-hydroxybenzoic acid + 3,5-dihydroxybenzoic acid); P_{COP}, p-hydroxybenzenes COP (p-hydroxybenzaldehyde+p-hydroxyacetophenone + p-hydroxybenzoic acid). Grab, Shipek grab sample; KC, kasten core sample; n.m., not measured. Station codes correspond to those in Figure 1. Coarse samples for which accurate SA measurements were not possible are indicated by <10 m^2/g.

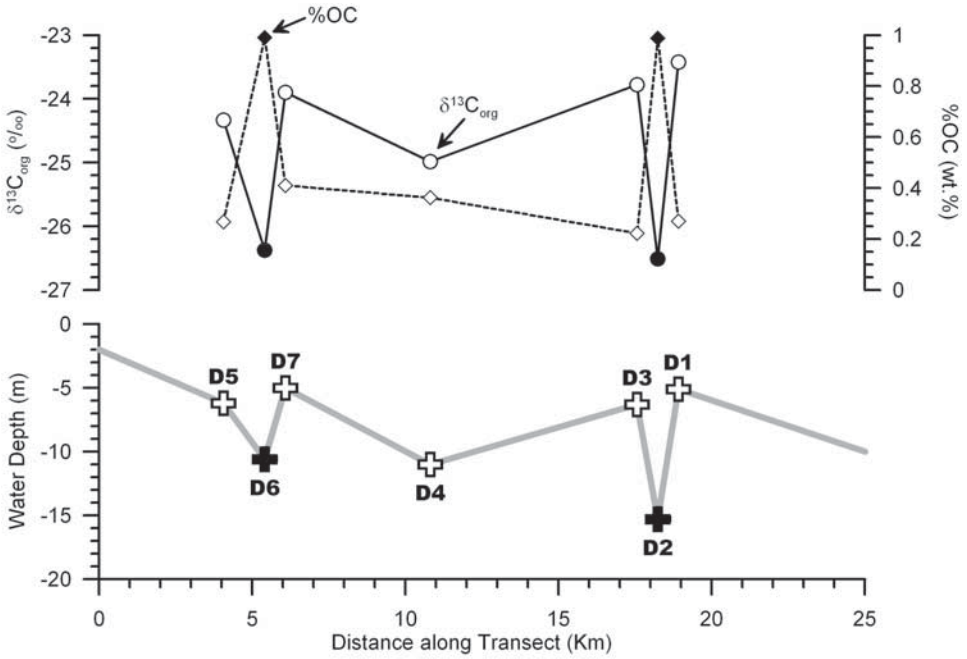

Figure 2. Compositions of surface sediments from the D station transect. The locations of the stations are highlighted within the square in Figure 1. The distance along the transect is measured from the tip of Kiwai Island (Figure 1). The data plotted include the stable carbon isotopic values of the organic matter ($\delta^{13}C_{org}$), the weight percent organic carbon content (%OC), and the water depth at each site.

values (0.08 wt %) than their counterparts from the other regions (0.10–0.11 wt %) whereas all of the low-SA samples displayed diminished %ON contents (0.03–0.04 wt %) relative to their high-SA counterparts. Inorganic carbon contents were low (<0.05 wt %) throughout the majority of the samples, with some evidence of textural differences among the SW region. However, the low contents and high variability make it difficult to assign statistical significance to these contrasts.

[23] Despite the contrasts in concentrations, there were no clear trends among OC:ON ratios from samples of different texture, with values ranging between 12 and 20 mol:mol for both high-SA and low-SA sediments. Notably, these values are all considerably higher than those of typical algal sources (i.e., Redfield ratio of 6–7 mol:mol). All the samples displayed stable carbon isotopic compositions that were depleted ($\delta^{13}C_{org} < -24$ ‰) relative to the typical marine values (−19 to −21 ‰) [e.g., *Fogel and Cifuentes*, 1993] and comparable to typical as well as local C_3 terrigenous sources (−25 to −29 ‰) [*Fogel and Cifuentes*, 1993; *Bird et al.*, 1994]. Notably, we observed significant differences between the $\delta^{13}C_{org}$ compositions of high-SA and low-SA sediments, with the former exhibiting depleted $\delta^{13}C_{org}$values (−26.5 to −25.8 ‰) relative to their low-SA counterparts (−24.6 to −24.1 ‰, respectively; Figure 3). In the case of $\delta^{15}N$ compositions, all samples displayed values ($\delta^{15}N < +2$ ‰) that were comparable to those of typical terrigenous sources of ON and depleted relative to typical $\delta^{15}N$ signatures of marine sources (+2 ‰ vs. +8 ‰, respectively) [e.g., *Fogel and Cifuentes*, 1993]. In two of the regions (Umuda Valley and NE), the low-SA sediments displayed $\delta^{15}N$ values that were enriched relative to their high-SA counterparts (Figure 3).

[24] Among the CuO oxidation products, the yields of vanillyl and syringyl phenols (V_{COP} and S_{COP}; respectively) were significantly elevated in the high-SA samples relative to their low-SA counterparts (Figure 4). The highest yields of these compounds were found in the NE and SW regions ($V_{COP} \sim 3$ mg (100 mg OC)$^{-1}$; $S_{COP} \sim 2$ mg (100 mg OC)$^{-1}$, with lower values in the Fly River and Umuda Valley sediments ($V_{COP} \sim 2$ mg (100 mg OC)$^{-1}$; $S_{COP} \sim$ 1.5 mg (100 mg OC)$^{-1}$)). In contrast, the yields of cinnamyl phenols (C_{COP}) were much more uniformly distributed (0.12–0.16 mg (100 mg OC)$^{-1}$) among high-SA samples. Furthermore, the low-SA sediments from the Umuda Valley and SW regions were characterized by comparable C_{COP} yields relative to their high-SA counterparts (Figure 4). There were significant differences in the yields of total lignin phenols (Λ_{COP}) among high-SA sediments, with the NE samples displaying the highest values ($\geq$5 mg (100 mg OC)$^{-1}$) and the Fly River sample the lowest ($\sim$3 mg (100 mg OC)$^{-1}$; Figure 4). All of the low-SA samples displayed much lower Λ_{COP} values ($\leq$1 mg (100 mg OC)$^{-1}$) relative to their high-SA counterparts. A similar overall pattern was detected for the nonlignin CuO products. For example, the highest yields of *p*-hydroxybenzene products (P_{COP}) were displayed by high-SA samples from the NE region (0.6 mg (100 mg OC)$^{-1}$), whereas the lowest values (<0.2 mg (100 mg OC)$^{-1}$) were detected in the low-SA samples. In the case of the other benzoic acid products (B_{COP}), although there were significant contrasts between the yields of high-SA and low-SA samples in the Umuda Valley and NE regions, they were not as marked as with other

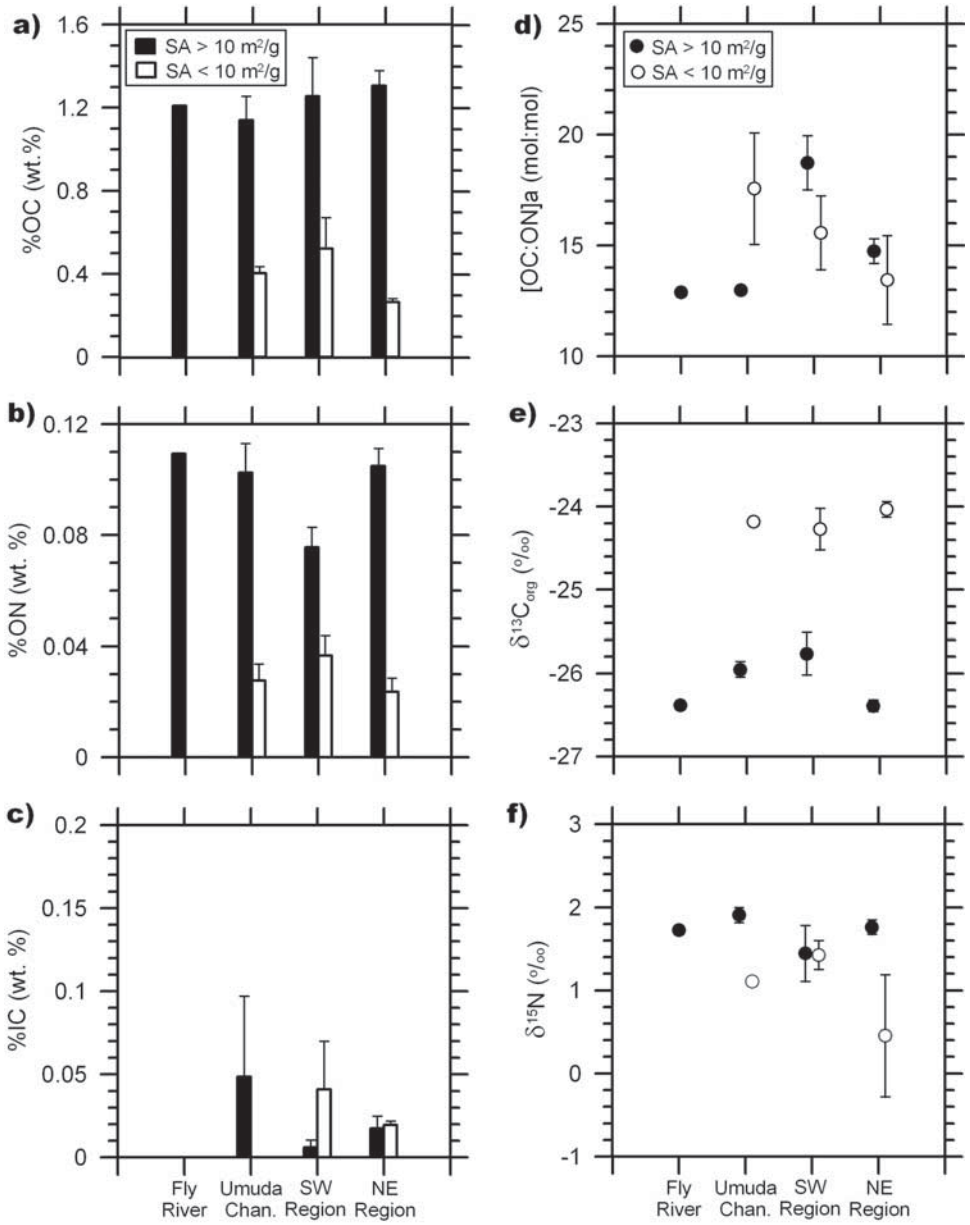

Figure 3. Average compositions of sediments from different geographical areas. Separate averages are computed for sediments of fine texture (surface area >10 m^2 g^{-1}, solid symbols) and for sediments of coarse texture (surface area <10 m^2 g^{-1}, open symbols). The parameters plotted include (a) weight percent organic carbon content (%OC), (b) weight percent organic nitrogen content (%ON), (c) weight percent inorganic carbon content (%IC), (d) molar OC:ON ratios, (e) stable carbon isotopic compositions of organic matter ($\delta^{13}C_{org}$), and (f) stable nitrogen isotopic compositions of total nitrogen ($\delta^{15}N$). Error bars indicate the variability (±1 standard error) within each site and sample type.

CuO products. Moreover, the yields of B_{COP} from high-SA and low-SA samples within the SW region were comparable. In this respect, the distribution of C_{COP} and B_{COP} among sample types was much more similar than for the rest of the CuO products (Figure 4).

[25] Overall, these results indicate that there were significant compositional differences between OM present in high-SA and low-SA samples. These differences included contrasts in the elemental concentrations (%OC, %N) and stable isotope ratios ($\delta^{13}C_{org}$, $\delta^{15}N$), as well as the yields and compositions of lignin and nonlignin oxidation products. Such contrasting patterns suggest samples of different textures contained OM with distinct sources and/or diagenetic histories. In order to further investigate the composition and sources of OM within the study area, we selected several samples of contrasting surface area (and hence texture) for density fractionation. Once fractionated into high- and low-density fractions, we measured the radiocarbon compositions of the OC in these different fractions (Table 2). According to these analyses all of the unfractio-

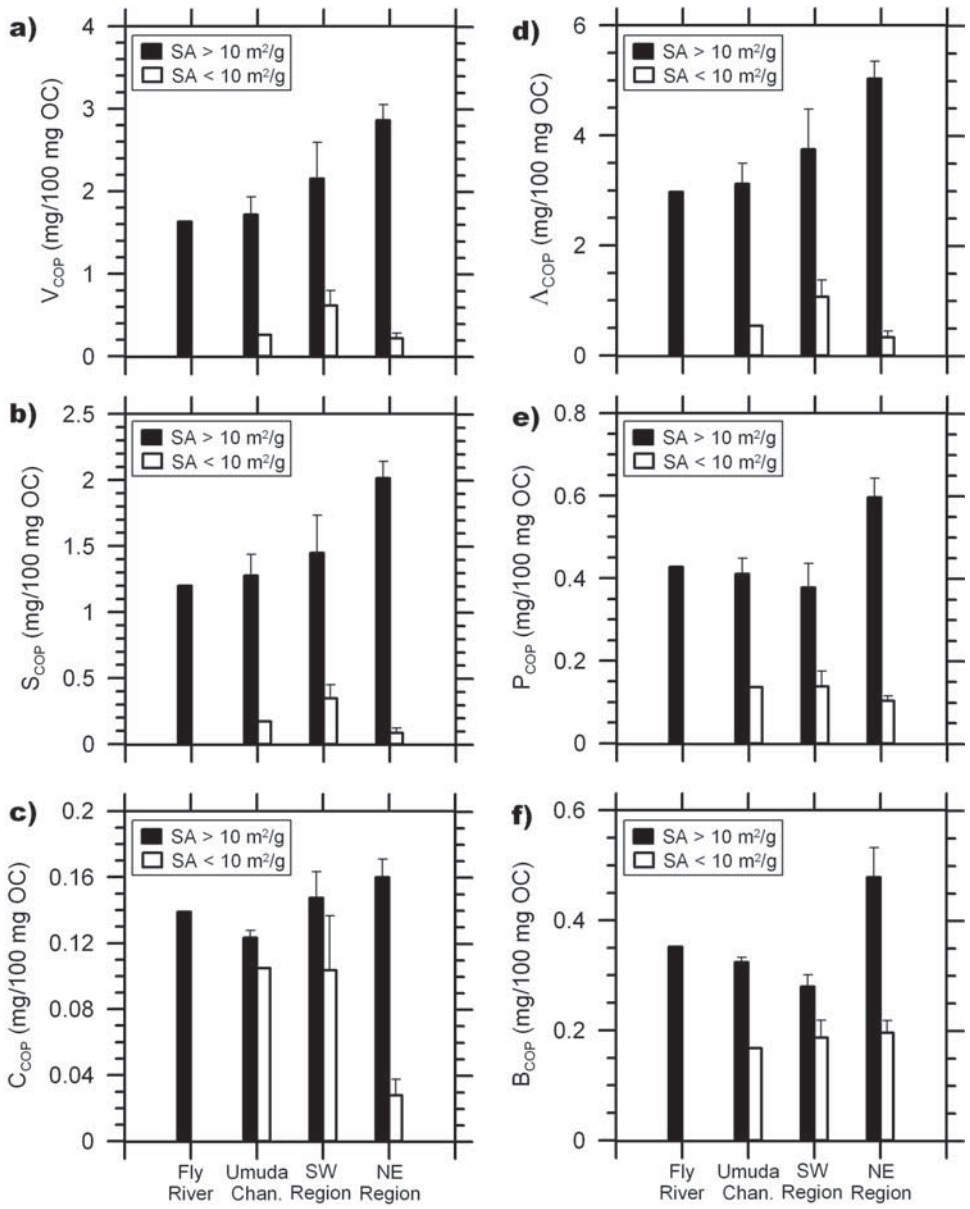

Figure 4. Average carbon-normalized yields (mg (100 mg OC) $^{-1}$) of lignin and nonlignin CuO oxidation products from different geographical areas. Separate averages are computed for sediments of fine texture (surface area >10 m^2 g^{-1}, solid bars) and for sediments of coarse texture (surface area <10 m^2 g^{-1}, open bars). The parameters plotted include the yields for different classes of lignin-derived CuO oxidation products such as (a) vanillyl products (V_{COP}), (b) syringyl products (S_{COP}), (c) cinnamyl products (C_{COP}), (d) sum of lignin products ($\Lambda_{COP} = V_{COP} + S_{COP} + C_{COP}$), (e) *p*-hydroxybenzene products (P_{COP}), and (f) other benzoic acid products (B_{COP}). Error bars indicate the variability (±1 standard error) within each site and sample type.

nated sediments contained OM that was depleted in ^{14}C, with $\Delta^{14}C_{org}$ values that ranged from −300 to less than −500 ‰. These $\Delta^{14}C_{org}$ values translate into age estimates of 2,800 to > 6,000 years before present (years B.P.) (Table 2).

[26] Measurements of the high-density fractions (>1.9 g cm^{-3}) indicate this material accounts for the majority (>70%) of the total carbon in the surface sediments and was characterized by $\Delta^{14}C_{org}$ values and ^{14}C ages that were significantly more depleted and older (−370 to −645 ‰ and 3,700 to >8,200 years B. P., respectively) than those found in the bulk sediments (Table 2). Notably, the $\delta^{13}C_{org}$ compositions of the high-density fractions were enriched by >1 ‰ relative to the values measured in the bulk sediments, and the OC:ON ratios were significantly lower than those from bulk sediments. In contrast, the low-density fractions typically accounted for a smaller fraction of the sedimentary OM and were characterized by higher OC:ON ratios and more depleted $\delta^{13}C_{org}$ compositions than their high-density counterparts. The $\Delta^{14}C_{org}$ values of the low-density samples,

Table 2. Compositions of Density-Fractionated, Surface Sediment Samples From Various Locations of the Fly River Delta[a]

		Inshore Northeast			Offshore Northeast		Umuda	Southwest	
Parameter	Units	CC5	EE5	FF3	BB9	CC9	C11	D2	E15
Unfractionated Sediments									
SA	m^2/g	22.9	20.2	25.6	17.7	15.0	25.7	10.4	14.6
%OC	wt %	1.6	1.3	1.2	1.2	0.82	1.3	1.1	1.2
[OC/ON]a	mol:mol	14	14	13	14	17	12	17	17
δ^{13}Corg	‰	−26.5	−26.4	−26.4	−26.2	−25.8	−26.0	−26.5	−26.3
Δ^{14}Corg	‰	−340.6	−343.1	−301.2	−401.5	−462.0	−388.8	−538.9	−492.9
Age	ybp	3290	3325	2825	4070	4925	3900	6165	5400
f−modern	fraction	0.66	0.66	0.70	0.60	0.54	0.62	0.46	0.51
High Density (>1.9 g/cm^3) Fraction									
Abundance	% of mass	57	56	47	88	70	89	90	89
%OC	wt %	1.1	0.55	0.95	0.76	0.35	0.87	0.66	0.61
[OC/ON]a	mol:mol	11	9	11	10	9	11	12	11
δ^{13}Corg	‰	−26.1	−24.8	−25.4	−24.4	−24.7	−24.1	−25.7	−24.7
Δ^{14}Corg	‰	−399.1	−520.4	−372.6	−500.0	−633.6	−413.5	−620.8	−643.5
Age	ybp	4040	5850	3690	5515	8010	4235	7735	8230
f−modern	fraction	0.60	0.48	0.63	0.50	0.37	0.59	0.38	0.36
Low Density (<1.9 g/cm^3) Fraction									
Abundance	% of mass	43	44	53	12	30	11	10	11
%OC	wt %	1.0	1.7	0.81	5.4	0.61	1.8	5.9	3.0
[OC/ON]a	mol:mol	15	15	15	24	28	20	29	26
δ^{13}Corg	‰	−26.9	−27.1	−27.5	−28.3	−27.3	−33.3	−27.4	−29.0
Δ^{14}Corg[b]	‰	−256.4	−269.5	−227.1	−279.0	−226.1	−295.6	−444.8	−238.0
Age	ybp	2579	2685	2359	2764	2351	2907	4585	2438
f−modern	fraction	0.74	0.73	0.77	0.72	0.77	0.70	0.56	0.76

[a]Surface is 0−2 cm. Column headings: SA, mineral surface area; %OC, weight percent organic carbon content; [OC:ON]a, atomic organic carbon:nitrogen ratio; δ^{13}Corg, stable isotopic ratio of organic carbon; Δ^{14}Corg, radiocarbon isotope ratio of organic carbon; Age, radiocarbon age in years before present (ybp) [*Stuiver and Polach*, 1977]; f-modern, radiocarbon concentration as fraction modern; Abundance, fraction of total mass in the sample as a percentage.

[b]Estimated by isotopic mass balance between unfractionated sediments and high-density fractions.

which were estimated by isotopic mass balance, indicate these materials were significantly younger than the high-density materials (Table 2). The contrasts between high- and low-density fractions were least pronounced in the samples from the inshore area of the NE region. Overall, these compositions suggest that there were significant differences in the composition and sources of OM among the two density classes, with older, N-enriched and ^{13}C-enriched materials contributing predominantly to the high-density fraction whereas younger, N-depleted and ^{13}C-depleted materials were more important in the low-density fraction. Likely sources for the high-density fractions include highly altered, old soil OM and/or fossil carbon eroded from bedrock, whereas vascular plant debris appears to be an important component of the low-density fractions.

[27] The isotopic compositions of individual lignin phenols from a selected set of samples (Table 3) show that all of the vanillyl and syringyl phenols yielded δ^{13}C compositions that were highly depleted, ranging from −27 to −32‰. These values are consistent with the compositions measured for C_3 vascular plant tissues [e.g., *Goni and Eglinton*, 1996] and indicate the predominant source of the lignin in these samples was C_3 land plants. There was no indication that C_4 grasses contributed any significant amount to the lignin present in the samples analyzed. Because of the low concentrations of lignin phenols in most low-SA samples, we

Table 3. Stable Carbon Isotopic Compositions of Individual Lignin CuO Oxidation Products From Surface Sediments[a]

Sample	Vl	Vn	Vd	Sl	Sn	Sd
Northeast region						
FF3 (0−1 cm)	−27.7 ± 0.4	−29.3 ± 0.3	−29.7 ± 1.1	−28.5 ± 0.4	−29.5 ± 0.5	−31.5 ± 0.6
EE5 (0−1 cm)	−29.2 ± n.a.	−29.9 ± n.a.	−34.5 ± n.a.	−29.5 ± n.a.	−31.0 ± n.a.	−33.2 ± n.a.
CC5 (0−1 cm)	−27.6 ± 0.0	−29.1 ± 0.0	−31.7 ± 0.0	−28.1 ± 0.0	−29.2 ± 0.0	−30.8 ± 0.0
BB9 (0−1 cm)	−27.1 ± 0.8	−28.0 ± 0.7	−29.5 ± 1.6	−26.9 ± 0.7	−28.4 ± 0.7	−28.0 ± 1.5
Northeast avg.	−27.9 ± 0.9	−29.1 ± 0.8	−31.4 ± 2.3	−28.2 ± 1.1	−29.5 ± 1.1	−30.9 ± 2.2
Umuda channel						
C11 (0−1 cm)	−27.1 ± 0.1	−28.2 ± 0.1	−30.3 ± 0.2	−27.6 ± 0.1	−29.2 ± 0.1	−29.2 ± 0.2
Southeast region						
D2 (0−1cm)	−27.9 ± 0.1	−29.0 ± 0.1	−33.6 ± 0.1	−28.1 ± 0.1	−29.1 ± 0.0	−31.1 ± 0.1
E15 (0−1 cm)	−26.8 ± 0.0	−28.1 ± 0.0	−29.0 ± 0.0	−27.1 ± 0.0	−28.3 ± 0.0	−29.2 ± 0.0
G3 (1−2 cm)	−28.2 ± 0.0	−29.7 ± 0.0	−31.0 ± 0.1	−28.1 ± 0.0	−28.9 ± 0.0	−31.7 ± 0.1
Southeast avg.	−27.5 ± 0.7	−28.7 ± 0.7	−31.0 ± 2.0	−27.7 ± 0.5	−28.9 ± 0.4	−30.3 ± 1.3

[a]Stable carbon isotopes, δ^{13}C, are given in ‰. Column headings: Vl, vanillin; Vn, acetovanillone; Vd, vanillic acid; Sl, syringealdehyde; Sn, acetosyringone; Sd, syringic acid; n.a., not applicable. The sample codes correspond to the station locations indicated in Figure 1. The interval depth (cm) is indicated within the parentheses.

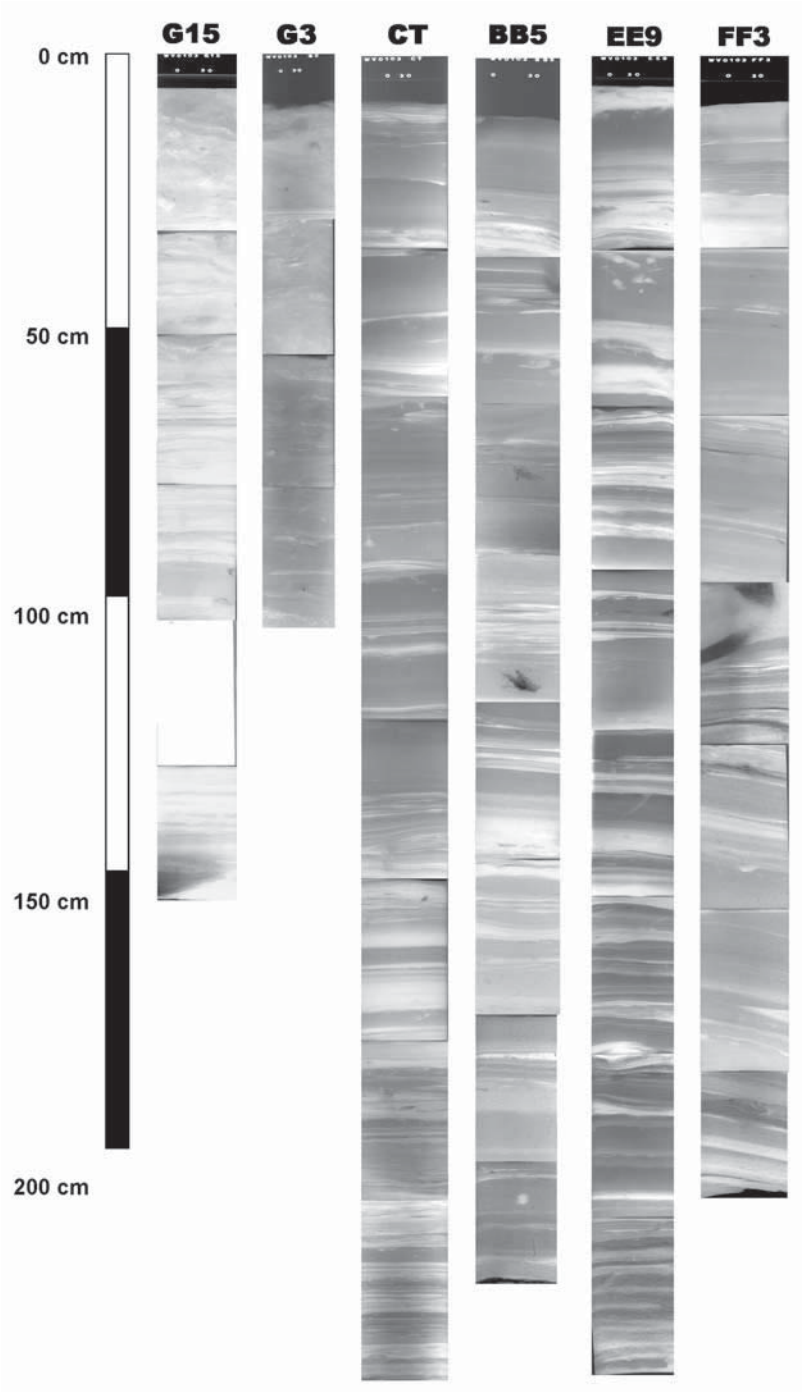

Figure 5. Composites of X-radiograph negatives from selected kasten cores. The white portion of G15 indicates that no radiograph was taken for this section of the core. Lighter tones reflect more X-ray opaque, coarser, sand-rich horizons, whereas dark tones are characteristic of fine sediments. The reason for the overall light colors for G15 is that the X rays were slightly overexposed.

were unable to measure their $\delta^{13}C$ compositions by IRM-GC-MS. Hence we cannot make a similar assessment for the lignin-bearing OM within these coarser deposits.

4.2. Down-Core Compositions

[28] In order to investigate the compositions of subsurface sediments within the delta-clinoform system, we analyzed several kasten cores collected from the NE, Umuda Valley and SW regions. These cores spanned the range of depositional environments along the study area. Mass accumulation rates, based on excess ^{210}Pb activity profiles, ranged from negligible in the SW region (G3, G15), to 1.3 g cm^{-2} a^{-1} in the Umuda Valley at the CT (i.e., Rusty Tripod) [*Ogston et al.*, 2007] site, to 2.6 g cm^{-2} a^{-1} in the inner area of the NE region directly offshore from the

Table 4. Compositions of Sediment Horizons From Selected Kasten Cores[a]

Interval, cm	SA, m^2/g	Percent ON, wt %	Percent OC, wt %	Percent IC, wt %	$\delta^{15}N$, ‰	$\delta^{13}C$, ‰	CuO Oxidation Product (COP) Yields, mg/100 mg OC				
							V_{COP}	S_{COP}	C_{COP}	B_{COP}	P_{COP}
FF3											
000–001	25.6	0.11	1.25	0.15	1.95	−26.4	2.61	1.74	0.121	0.463	0.675
001–002	24.4	0.13 ± 0.002	1.42 ± 0.02	0.00 ± 0.02	1.75 ± 0.20	−26.4 ± 0.0	2.63 ± 0.06	2.18 ± 0.04	0.140 ± 0.018	0.417 ± 0.046	0.674 ± 0.030
005–006	25.6	0.13 ± 0.000	1.46 ± 0.01	0.00 ± 0.01	1.77 ± 0.21	−26.3 ± 0.0	n.m.	n.m.	n.m.	n.m.	n.m.
010–011	30.6	0.14	1.41	0.00	n.m.	n.m.	2.74	1.70	0.164	0.420	0.618
014–015	25.3	0.15	1.36	0.00	1.30	−26.0	n.m.	n.m.	n.m.	n.m.	n.m.
019–020	25.6	0.13	1.36	0.00	1.96	−26.2	n.m.	n.m.	n.m.	n.m.	n.m.
024–026	26.2	0.12	1.25	0.00	2.62	−26.1	2.32	1.56	0.225	0.494	0.718
030–032	28.1	0.12	1.26	0.00	1.84	−26.2	n.m.	n.m.	n.m.	n.m.	n.m.
034–036	31.3	0.12	1.18	0.00	1.76	−26.0	2.04	1.97	0.166	0.470	0.596
040–042	28.8	0.11	1.19	0.00	1.87	−26.2	n.m.	n.m.	n.m.	n.m.	n.m.
044–046	27.6	0.13	1.34	0.03	1.76	−26.4	n.m.	n.m.	n.m.	n.m.	n.m.
050–052	25.8	0.12	1.33	0.00	2.00	−26.2	n.m.	n.m.	n.m.	n.m.	n.m.
058–060	22.7	0.12	1.27	0.00	1.85	−26.3	n.m.	n.m.	n.m.	n.m.	n.m.
070–072	16.8	0.16	3.23	0.00	1.90	−27.0	7.65 ± 0.48	5.58 ± 0.85	0.295 ± 0.033	0.646 ± 0.092	1.397 ± 0.022
078–080	14.9	0.12	2.05	0.00	n.m.	n.m.	5.77	3.77	0.265	0.447	0.955
092–094	17.7	0.11	1.22	0.03	1.79	−26.4	3.41	2.41	0.268	0.520	0.735
100–102	23.8	0.10 ± 0.000	1.32 ± 0.02	0.00 ± 0.02	2.45 ± 0.27	−26.7 ± 0.1	n.m.	n.m.	n.m.	n.m.	n.m.
118–120	21.2	0.08	1.07	0.05	2.16	−26.8	5.91	2.86	0.167	0.411	0.581
130–132	15.8	0.08	0.84	0.07	1.80	−26.3	3.20	2.02	0.084	0.505	0.695
142–144	22.8	0.12	1.33	0.00	1.90	−26.6	n.m.	n.m.	n.m.	n.m.	n.m.
148–150	20.5	0.12	1.33	0.00	2.73	−26.6	n.m.	n.m.	n.m.	n.m.	n.m.
160–162	16.4	0.11	1.80	0.06	2.01	−26.9	5.19	3.00	0.237	0.498	0.951
172–174	15.6	0.10	1.31	0.01	2.38	−26.5	3.83	2.62	0.166	0.448	0.755
178–180	17.6	0.08	1.03	0.07	1.98	n.m.	3.82	2.31	0.130	0.519	0.805
190–192	13.1	0.08	0.92	0.02	1.88	−26.6	n.m.	n.m.	n.m.	n.m.	n.m.
200–202	20.2	0.07 ± 0.000	0.70 ± 0.00	0.08 ± 0.00	1.55 ± 0.08	−26.7 ± 0.3	2.31 ± 0.06	1.45 ± 0.09	0.071 ± 0.002	0.474 ± 0.027	0.504 ± 0.038
EE9											
000–001	11.8	0.07	1.17	0.00	0.92	−26.6	3.05	1.56	0.107	0.295	0.577
001–002	14.1	0.06	0.97	0.00	1.27	−26.4	3.83	2.18	0.164	0.325	0.600
005–006	15.7	0.05	0.33	0.04	1.56	−25.0	n.m.	n.m.	n.m.	n.m.	n.m.
010–011	28.4	0.09	0.80	0.00	2.21	−25.5	n.m.	n.m.	n.m.	n.m.	n.m.
015–016	21.9	0.08	0.55	0.00	2.12	−25.0	n.m.	n.m.	n.m.	n.m.	n.m.
020–022	20.9	0.05 ± 0.008	0.54 ± 0.05	0.00 ± 0.05	2.12 ± 0.15	−25.7 ± 0.1	n.m.	n.m.	n.m.	n.m.	n.m.
024–026	22.2	0.06	0.51	0.02	−0.42	−25.5	1.46	0.67	0.060	0.338	0.317
030–032	n.m.	0.12	1.29	0.01	1.85	−26.6	n.m.	n.m.	n.m.	n.m.	n.m.
034–036	26.7	0.10	1.28	0.00	0.96	−26.6	n.m.	n.m.	n.m.	n.m.	n.m.
038–040	n.m.	0.10	1.01	0.00	n.m.	−26.3	n.m.	n.m.	n.m.	n.m.	n.m.
044–046	32.4	0.08	0.74	0.00	1.76	−26.1	n.m.	n.m.	n.m.	n.m.	n.m.
050–052	n.m.	0.05	0.37	0.07	2.34	−25.1	n.m.	n.m.	n.m.	n.m.	n.m.
058–060	25.4	0.08	0.94	0.05	2.53	−26.5	n.m.	n.m.	n.m.	n.m.	n.m.
070–072	n.m.	0.07	0.60	0.07	2.79	−25.9	n.m.	n.m.	n.m.	n.m.	n.m.
078–080	30.2	0.10	1.06	0.00	2.26	−26.5	n.m.	n.m.	n.m.	n.m.	n.m.
090–092	n.m.	0.14	1.91	0.06	2.60	−26.9	n.m.	n.m.	n.m.	n.m.	n.m.
098–100	27.0	0.09 ± 0.005	2.15 ± 0.10	0.00 ± 0.10	2.55 ± 0.39	−27.3 ± 0.1	9.18	2.05	0.249	1.402	1.910
108–110	n.m.	0.13	1.68	0.00	1.88	−26.7	4.73	2.11	0.439	1.053	0.916
120–122	33.0	0.12	1.21	0.09	3.07	−26.2	n.m.	n.m.	n.m.	n.m.	n.m.
138–140	15.8	0.05	0.31	0.03	2.39	−25.0	n.m.	n.m.	n.m.	n.m.	n.m.
150–152	28.2	0.06	0.65	0.00	2.47	−26.6	3.74	1.78	0.461	1.035	0.856

Table 4. (continued)

Interval, cm	SA, m^2/g	Percent ON, wt %	Percent OC, wt %	Percent IC, wt %	$\delta^{15}N$, ‰	$\delta^{13}C$, ‰	CuO Oxidation Product (COP) Yields, mg/100 mg OC				
							V_{COP}	S_{COP}	C_{COP}	B_{COP}	P_{COP}
168–170	n.m.	0.10	1.01	0.10	n.m.	n.m.	n.m.	n.m.	n.m.	n.m.	n.m.
180–182	16.1	0.05	0.34	0.01	2.98	−25.4	n.m.	n.m.	n.m.	n.m.	n.m.
198–200	n.m.	0.12	1.13	0.05	2.87	−26.3	2.77	1.41	0.146	0.991	0.802
210–212	19.3	0.08	0.74	0.09			n.m.	n.m.	n.m.	n.m.	n.m.
240–242	29.4	0.07 ± 0.000	0.56 ± 0.01	0.11 ± 0.01	2.82 ± 0.17	−25.7 ± 0.1	4.04 ± 0.05	2.44 ± 0.26	0.475 ± 0.135	1.387 ± 0.208	0.917 ± 0.312
BB5											
000–001	19.3	0.13	1.60	0.07	1.54 ± 0.37	−26.8 ± 0.0	3.88	2.61	0.260	0.435	0.985
001–002	20.9	0.12	1.55	0.00	2.21 ± 0.19	−26.6 ± 0.1	3.27	2.17	0.192	1.285	0.749
002–003	24.0	0.11	1.44	0.10	1.40	−26.5	n.m.	n.m.	n.m.	n.m.	n.m.
005–006	n.m.	0.16	2.42	0.12	1.97	−27.0	4.25	1.81	0.212	0.471	0.844
009–010	23.5	0.14	2.05	0.03	1.19	−26.8	n.m.	n.m.	n.m.	n.m.	n.m.
015–016	n.m.	0.14	1.47	0.02	1.55	−26.5	n.m.	n.m.	n.m.	n.m.	n.m.
020–022	18.3	0.06 ± 0.001	0.58 ± 0.02	0.05 ± 0.02	2.33 ± 0.34	−26.2 ± 0.3	6.55 ± 1.04	3.04 ± 0.89	0.217 ± 0.014	1.096 ± 0.034	1.624 ± 0.188
024–026	n.m.	0.09	1.10	0.13	2.15	−26.7	n.m.	n.m.	n.m.	n.m.	n.m.
028–030	25.8	0.13	1.43	0.03	1.75	−26.6	n.m.	n.m.	n.m.	n.m.	n.m.
034–036	n.m.	0.10	1.35	0.08	1.71	−26.9	4.54	2.68	0.209	0.449	0.952
040–042	25.0	0.12	1.15	0.05	n.m.	n.m.	n.m.	n.m.	n.m.	n.m.	n.m.
044–046	n.m.	0.09	0.79	0.11	1.93	−25.9	n.m.	n.m.	n.m.	n.m.	n.m.
050–052	24.5	0.13	1.21	0.00	2.54	−26.3	3.09	2.18	0.132	0.399	0.641
058–060	n.m.	0.14	1.53	0.06	2.51	−26.7	n.m.	n.m.	n.m.	n.m.	n.m.
070–072	22.3	0.13	1.26	0.00	2.31	−26.5	n.m.	n.m.	n.m.	n.m.	n.m.
078–080	n.m.	0.12	1.46	0.05	1.83	−26.5	n.m.	n.m.	n.m.	n.m.	n.m.
090–092	23.6	0.14	1.16	0.07	3.01	−26.2	2.23	1.46	0.220	0.444	0.557
098–100	n.m.	0.10 ± 0.001	1.35 ± 0.05	0.00 ± 0.05	2.73	−26.9	4.38 ± 0.45	2.93 ± 0.38	0.190 ± 0.016	0.415 ± 0.030	0.868 ± 0.044
110–112	21.6	0.13 ± 0.000	1.34 ± 0.00	0.06 ± 0.00	3.06	−26.4	n.m.	n.m.	n.m.	n.m.	n.m.
118–120	n.m.	0.07	0.68	0.32	3.05	−26.5	n.m.	n.m.	n.m.	n.m.	n.m.
140–142	8.7	0.06	0.48	0.05	2.70	−26.6	1.68	1.14	0.087	0.335	0.349
150–152	11.2	0.05	0.45	0.05	2.25	−26.4	n.m.	n.m.	n.m.	n.m.	n.m.
160–162	n.m.	0.12	1.34	0.10	2.44	−26.8	3.17	2.24	0.151	0.436	0.622
170–172	25.3	0.13	1.40	0.03	3.16	−26.5	n.m.	n.m.	n.m.	n.m.	n.m.
180–182	n.m.	0.13	1.42	0.05	2.70	−26.5	n.m.	n.m.	n.m.	n.m.	n.m.
190–192	21.0	0.11	1.18	0.02	2.49	−26.4	n.m.	n.m.	n.m.	n.m.	n.m.
200–202	n.m.	0.12	1.42	0.03	2.03	−26.5	3.22	2.02	0.301	0.477	0.659
210–212	20.1	0.09	1.09	n.m.	2.38	−26.5	n.m.	n.m.	n.m.	n.m.	n.m.
220–222	20.9	0.11 ± 0.003	1.03 ± 0.02	0.12 ± 0.02	3.24 ± 0.23	−26.1 ± 0.0	n.m.	n.m.	n.m.	n.m.	n.m.
230–232	22.3	0.09	1.07	0.12	2.34	−26.5	3.26	1.96	0.112	0.483	0.595
CT											
000–001	20.6	0.10	1.25	0.00	1.46	−26.3	n.m.	n.m.	n.m.	n.m.	n.m.
001–002	16.5	0.09	0.92	0.04	1.99	−26.0	2.14	1.54	0.132	0.336	0.507
005–006	n.m.	0.10 ± 0.003	0.91 ± 0.01	0.09 ± 0.01	2.42	−25.9	n.m.	n.m.	n.m.	n.m.	n.m.
010–011	28.4	0.14	1.40	0.05	2.31	−26.4	2.41	1.98	0.176	0.433	0.672
015–016	n.m.	0.11	1.04	0.09	1.85	−26.1	n.m.	n.m.	n.m.	n.m.	n.m.
020–022	n.m.	0.13	1.28	0.02	1.91	−26.0	n.m.	n.m.	n.m.	n.m.	n.m.
024–026	31.0	0.13	1.36	0.03	2.00	−26.1	5.85	3.42	0.152	1.194	1.502
034–036	n.m.	0.13	1.42	0.02	2.19	−26.4	n.m.	n.m.	n.m.	n.m.	n.m.
040–042	29.8	0.11	1.05	0.08	2.34	−26.1	5.66	3.44	0.184	1.486	1.718
044–046	n.m.	0.14	1.50	0.03	2.56	−26.6	n.m.	n.m.	n.m.	n.m.	n.m.
058–060	n.m.	0.11	1.15	n.m.	1.99	−26.3	n.m.	n.m.	n.m.	n.m.	n.m.
070–072	n.m.	0.13	1.32	0.07	2.32	−26.2	n.m.	n.m.	n.m.	n.m.	n.m.

Table 4. (continued)

Interval, cm	SA, m^2/g	Percent ON, wt %	Percent OC, wt %	Percent IC, wt %	$\delta^{15}N$, ‰	$\delta^{13}C$, ‰	CuO Oxidation Product (COP) Yields, mg/100 mg OC				
							V_{COP}	S_{COP}	C_{COP}	B_{COP}	P_{COP}
088–090	28.7	0.11	1.04	0.09	1.45	−26.3	5.45	3.52	0.214	1.206	1.302
100–102	n.m.	0.10	0.95	0.13	2.85	−26.0	n.m.	n.m.	n.m.	n.m.	n.m.
118–120	n.m.	0.11	1.00	0.13	3.03	−26.0	n.m.	n.m.	n.m.	n.m.	n.m.
130–132	29.8	0.11 ± 0.006	1.03 ± 0.01	0.10 ± 0.01	2.54 ± 0.36	−25.8 ± 0.1	3.86 ± 0.50	1.95 ± 0.19	0.128 ± 0.066	0.928 ± 0.059	1.284 ± 0.142
148–150	n.m.	0.06	0.45	0.19	2.39	−25.6	n.m.	n.m.	n.m.	n.m.	n.m.
160–162	32.5	0.08	0.80	0.18	2.54	−25.9	4.03	2.55	0.125	0.883	0.936
170–172	32.2	0.06	0.49	0.14	2.70	−25.4	2.01	1.00	0.047	0.816	0.604
200–202	29.0	0.09	1.12	0.00	2.07	−26.6	3.43	2.19	0.198	0.423	0.667
218–220	n.m.	0.07	0.70	0.53	2.35	−26.4	n.m.	n.m.	n.m.	n.m.	n.m.
230–232	29.6	0.08 ± 0.000	0.81 ± 0.03	0.09	3.12	−26.2	1.82 ± 0.45	1.38 ± 0.27	0.082 ± 0.035	0.410 ± 0.016	0.421 ± 0.030
248–250	31.1	0.07	0.96	0.03	2.42	−26.5	7.84	4.39	0.266	1.323	1.544
G3											
000–001	15.6	0.09	1.44	0.00	2.20	−26.1	2.24	1.58	0.108	0.234	0.278
001–002	16.4	0.08 ± 0.003	1.30 ± 0.02	0.00 ± 0.02	2.16 ± 0.16	−25.8 ± 0.2	2.17 ± 0.20	1.41 ± 0.13	0.114 ± 0.030	0.268 ± 0.010	0.307 ± 0.021
005–006	n.m.	0.08	0.93	0.26	2.87	−26.2	n.m.	n.m.	n.m.	n.m.	n.m.
009–010	22.6	0.10	1.23	0.09	2.67	−26.0	3.11	2.40	0.295	1.070	0.338
014–015	n.m.	0.10	1.23	0.18	2.45	−26.5	n.m.	n.m.	n.m.	n.m.	n.m.
020–022	18.5	0.08	1.07	0.07	2.08	−26.6	n.m.	n.m.	n.m.	n.m.	n.m.
024–026	19.6	0.11	1.07	0.14	2.16	−26.3	6.41	3.23	0.513	0.975	1.126
030–032	n.m.	0.09	1.14	0.07	2.51	−26.4	n.m.	n.m.	n.m.	n.m.	n.m.
034–036	20.1	0.12	1.55	0.12	2.30	−26.8	12.01	6.15	0.541	1.452	1.823
038–040	n.m.	0.12	1.32	0.12	1.83	−26.6	n.m.	n.m.	n.m.	n.m.	n.m.
044–046	18.2	0.11 ± 0.015	1.00 ± 0.02	1.06 ± 0.03	2.66 ± 0.05	−25.8 ± 0.1	6.04 ± 1.12	3.59 ± 0.50	0.328 ± 0.047	1.180 ± 0.061	1.206 ± 0.250
050–052	n.m.	0.08	1.02	0.10	1.72	−26.4	n.m.	n.m.	n.m.	n.m.	n.m.
058–060	n.m.	0.12	1.40	0.04	2.39	−26.5	n.m.	n.m.	n.m.	n.m.	n.m.
070–072	21.3	0.09	1.17	0.10	2.46	−26.4	n.m.	n.m.	n.m.	n.m.	n.m.
078–080	n.m.	0.10	1.04	0.05	2.73	−26.2	n.m.	n.m.	n.m.	n.m.	n.m.
090–092	17.2	0.12	1.56	0.15	2.03	−27.0	13.49	6.74	0.755	1.631	2.160
098–100	n.m.	0.12	1.33	0.06	2.86	−26.7	n.m.	n.m.	n.m.	n.m.	n.m.
108–110	21.3	0.11 ± 0.015	0.95 ± 0.02	0.10 ± 0.03	2.98 ± 0.14	−26.0 ± 0.1	4.57 ± 0.25	2.00 ± 0.51	0.161 ± 0.053	0.915 ± 0.076	0.847 ± 0.201
120–122	17.7	0.11	1.42	0.07	2.95	−26.7	n.m.	n.m.	n.m.	n.m.	n.m.
132–134	n.m.	0.09	0.94	0.12	2.05	−26.1	n.m.	n.m.	n.m.	n.m.	n.m.
138–140	n.m.	0.09	1.07	0.25	2.39	−26.2	n.m.	n.m.	n.m.	n.m.	n.m.
150–152	18.6	0.09	1.06	0.08	2.34	−26.4	n.m.	n.m.	n.m.	n.m.	n.m.
G15											
000–001	16.9	0.09 ± 0.003	1.60 ± 0.08	0.00 ± 0.08	2.61	−24.6	1.10	0.80	0.099	0.170	0.204
001–002	22.9	0.10 ± 0.002	1.60 ± 0.04	0.00 ± 0.04	2.20	−24.8	0.91 ± 0.02	0.62 ± 0.06	0.088 ± 0.021	0.215 ± 0.012	0.244 ± 0.015
005–006	n.m.	0.10	0.91	0.58	2.92	−25.1	n.m.	n.m.	n.m.	n.m.	n.m.
010–011	n.m.	0.08	0.78	1.69	2.95	−24.7	2.59	2.00	0.442	0.900	0.788
015–016	22.9	0.09	0.96	0.63	3.06	−25.6	n.m.	n.m.	n.m.	n.m.	n.m.
020–022	n.m.	0.09	0.92	0.76	2.65	−25.7	n.m.	n.m.	n.m.	n.m.	n.m.
030–032	21.4	0.09 ± 0.000	0.99 ± 0.01	0.20	2.02 ± 0.39	−26.1 ± 0.1	2.61	1.60	0.316	0.852	0.678
036–038	n.m.	0.08	0.90	0.21	2.80	−26.1	n.m.	n.m.	n.m.	n.m.	n.m.
040–042	n.m.	n.m.	n.m.	1.47	n.m.	−25.5	n.m.	n.m.	n.m.	n.m.	n.m.
044–046	n.m.	0.09	1.00	0.20	3.24	n.m.	n.m.	n.m.	n.m.	n.m.	n.m.
046–048	n.m.	0.09	0.95	0.49	1.89	−25.6	n.m.	n.m.	n.m.	n.m.	n.m.
048–050	n.m.	0.09	0.95	0.78	2.69	−26.0	n.m.	n.m.	n.m.	n.m.	n.m.
058–060	21.0	0.09	0.89	0.26	1.81	−26.0	3.69	1.96	0.731	1.293	0.883
066–068	n.m.	0.09	0.94	0.27	1.78	−26.0	n.m.	n.m.	n.m.	n.m.	n.m.
078–080	23.1	0.08	0.79	0.12	3.02	−25.9	4.10	1.91	0.063	1.143	1.060

Table 4. (continued)

							CuO Oxidation Product (COP) Yields, mg/100 mg OC				
Interval, cm	SA, m^2/g	Percent ON, wt %	Percent OC, wt %	Percent IC, wt %	$\delta^{15}N$, ‰	$\delta^{13}C$, ‰	V_{COP}	S_{COP}	C_{COP}	B_{COP}	P_{COP}
090–092	20.8	0.12	1.60	0.10	2.13	−26.8	7.21 ± 0.52	4.22 ± 0.56	0.263 ± 0.028	1.132 ± 0.052	1.475 ± 0.114
098–100	n.m.	0.08	0.84	0.25	3.18	−26.1	n.m.	n.m.	n.m.	n.m.	n.m.
110–112	n.m.	0.10	1.18	0.08	1.66	−26.2	n.m.	n.m.	n.m.	n.m.	n.m.
116–118	n.m.	0.09 ± 0.000	1.05 ± 0.02	0.15 ± 0.02	2.27 ± 0.58	−26.1 ± 0.1	3.97	2.53	0.448	0.803	0.682
128–130	n.m.	0.09	1.01	0.23	1.76	−26.1	n.m.	n.m.	n.m.	n.m.	n.m.
140–142	23.8	0.09	1.08	0.08	2.77	−26.4	6.61	3.57	0.569	1.331	1.410
152–154	n.m.	0.09	0.99	0.15	2.25	−26.2	n.m.	n.m.	n.m.	n.m.	n.m.
158–160	n.m.	0.07	0.73	0.16	2.48	−26.0	n.m.	n.m.	n.m.	n.m.	n.m.
168–170	n.m.	0.10	1.08	0.28	2.76	−26.0	n.m.	n.m.	n.m.	n.m.	n.m.
180–182	18.0	0.09	0.95	0.19	2.19	−26.3	5.17	4.14	0.537	1.413	0.650
192–194	n.m.	0.08	0.81	0.23	2.10	−26.2	n.m.	n.m.	n.m.	n.m.	n.m.
198–200	n.m.	0.08	0.78	0.35	1.81	−25.7	n.m.	n.m.	n.m.	n.m.	n.m.
210–212	20.4	0.09	1.04	0.16	2.33	−26.2	6.15	2.97	0.097	1.100	1.285
222–224	n.m.	0.08	0.73	0.14	2.27	−25.5	n.m.	n.m.	n.m.	n.m.	n.m.
228–230	n.m.	0.09	0.93	0.19	3.00	−26.0	n.m.	n.m.	n.m.	n.m.	n.m.
240–242	20.1	0.11	0.88	0.41	2.50	−25.7	4.57	3.63	0.433	1.413	0.612
252–254	18.9	0.09 ± 0.006	0.82 ± 0.02	0.46 ± 0.02	3.20 ± 0.11	−25.4 ± 0.0	4.04 ± 0.28	2.23 ± 0.42	0.182 ± 0.045	0.966 ± 0.139	0.983 ± 0.104

[a]Column headings: SA, mineral surface area; %ON, wt.% organic nitrogen; %OC, wt.% organic carbon; %IC, wt.% inorganic carbon; V_{COP}, vanillyl CuO oxidation products (vanillin + acetovanillone + vanillic acid); S_{COP}, syringyl COP (syringealdehyde + acetosyringone + syringic acid); C_{COP}, cinnamyl COP (p-coumaric acid + ferulic acid); B_{COP}, benzoic acid COP (benzoic acid+m-hydroxybenzoic acid + 3,5-dihydroxybenzoic acid); P_{COP}, p-hydroxybenzenes COP (p-hydroxybenzaldehyde + p-hydroxyacetophenone + p-hydroxybenzoic acid). Grab, Shipek grab sample; KC, kasten core sample; n.m., not measured. Station codes correspond to those in Figure 1.

northern distributary at site BB5. Accumulation rates were significantly lower ($\leq$0.5 g cm^{-2} a^{-1}) in the more distal areas of the NE region (FF3 and EE9 sites). Details on the ^{210}Pb profiles and their interpretation are provided elsewhere [*Crockett*, 2006; *Crockett et al.*, 2008].

[29] Figure 5 shows a composite of the X-radiographs taken from the sections of these kasten cores. All the cores displayed abundant horizontal layering made up of sediment packages of contrasting grain size. In these X-radiograph negatives, lighter areas reflect more X-ray opaque, coarser, sand-rich horizons, whereas fine sediments show as dark tones. The type of layering exhibited by these cores has been observed by other investigators [e.g., *Harris et al.*, 1993] and is thought to be caused by sedimentation, resuspension and winnowing processes associated with changes in sediment flux, tidal currents and wave energy. Changes in the thickness and abundance of the layers reflect variability in these processes over the depositional history of the cores.

[30] Another important corollary of the ubiquitous layering is the limited bioturbation observed throughout most of the cores. The processes that lead to these types of structures are characteristic of high-sedimentation/high-energy environments that limit the establishment of macrofauna capable of bioturbating the sediment and disrupting the layers [e.g., *Nittrouer and Sternberg*, 1981]. The only major signs of bioturbated sediments were observed in the top layers of G15 and G2 cores, which displayed mottled structures characteristic of biological activity. These features suggest that the delivery of sediment to this region may have been diminished over the recent history of these two cores, allowing fauna to colonize the top horizons of the seabed [see *Martin et al.*, 2007]. Notably, bioturbated layers were absent in the surfaces of other cores, indicating both the supply of sediment and the physical processes responsible for the layers were active in most other locations [e.g., *Crockett et al.*, 2008]. We found no visible evidence (e.g., high porosity, disturbed horizons) that would point to methanic conditions in the cores analyzed.

[31] All the geochemical data on the down-core compositions of the selected kasten cores are presented in Table 4. The compositional parameters determined for these samples included SA, %OC, %ON, %IC, $\delta^{15}N$ and $\delta^{13}C_{org}$, as well as the yields of lignin and nonlignin COP. Overall, most down-core profiles were characterized by fairly uniform compositions (e.g., Figures 6 and 7). For all of the parameters measured, there were no consistent trends with depth indicative of steady state diagenesis or long-term changes in sediment and OM supply. For example, none of the cores displayed decreases in %OC or in Λ_{COP} with increasing depth that would be expected if in situ OM degradation rates were at steady state. Furthermore, there were no clear trends in the OC:ON or $\delta^{13}C_{org}$ distributions down core, which could be interpreted as marked changes in the composition of OM deposited at each site. Instead, most of the down-core variability was associated with the heterogeneity of specific horizons, which were related to the variations in grain size of individual layers as evident in the X radiographs.

[32] There were statistically significant differences among the average compositions of the kasten cores from the different sites (Figure 8). For example, the highest SA

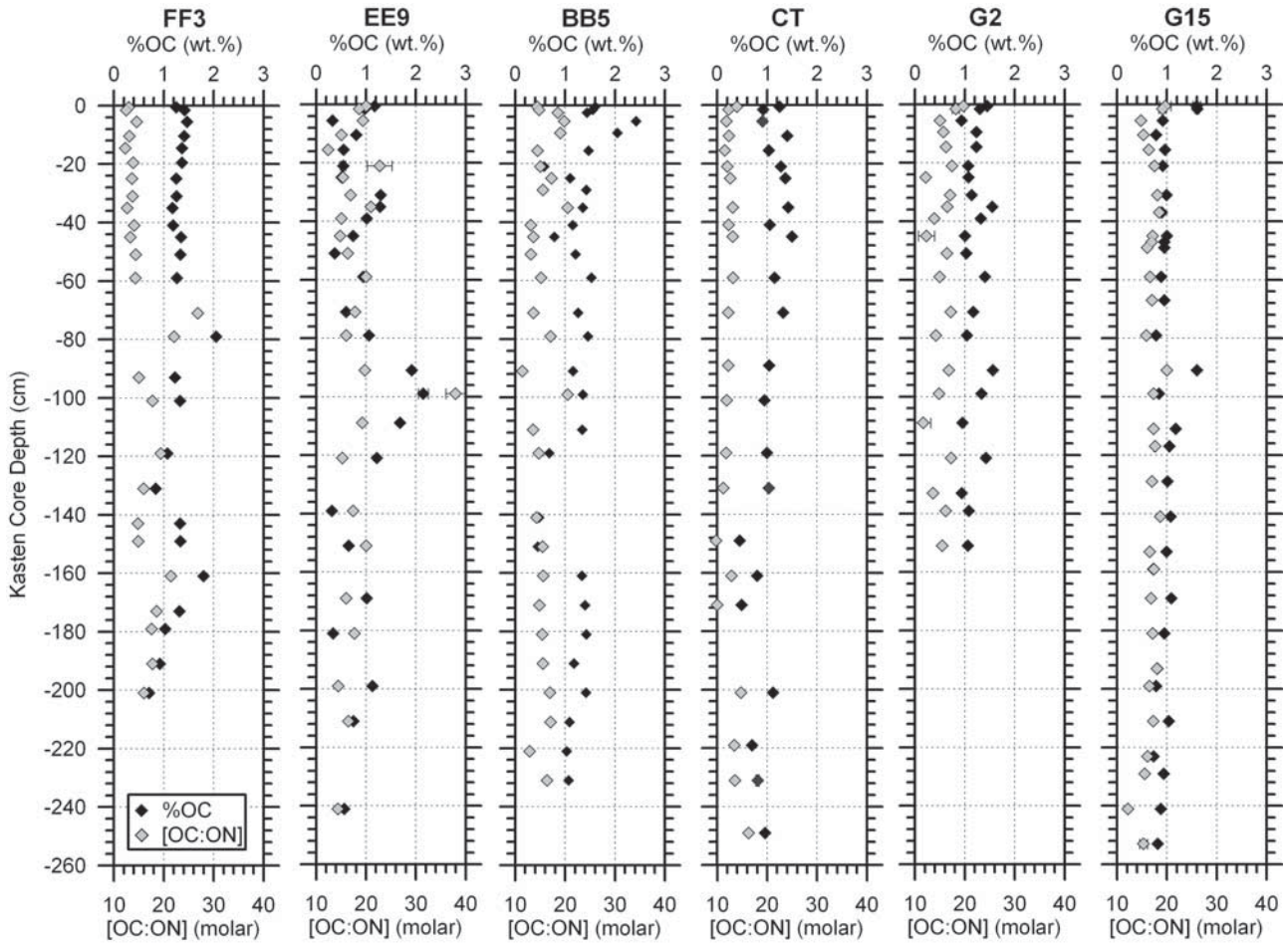

Figure 6. Down-core profiles of organic carbon contents (%OC) and molar organic carbon:nitrogen ratio (OC:ON) from selected kasten cores.

values characterized the site within the Umuda Valley (CT), whereas the inshore site from the SW region of the delta (G2) displayed the lowest SA values. Significant differences were also observed among the %OC contents of the cores, with EE9 displaying the lowest values. The cores from the SW region (G2 and G15) were characterized by elevated %IC contents relative to their counterparts in the NE region. The CT site also displayed the lowest OC:ON ratios, whereas the $\delta^{15}N$ and $\delta^{13}C_{org}$ compositions of the NE cores were generally depleted relative to the values displayed by their SW counterparts. The cores from the inner NE shelf region (FF3 and BB5) were characterized by low yields of Λ_{COP}, P_{COP} and B_{COP} relative to their counterparts in the SW region. These contrasts indicate that there was significant compositional heterogeneity in the sedimentary OM buried within the different regions of the Fly delta-clinoform system.

5. Discussion

5.1. Sources of OM in Surface and Subsurface Sediments

5.1.1. Insights From Isotope Data

[33] Our results reveal significant compositional differences between OM present in sediments of contrasting texture, as well as between the low- and high-density fractions of sedimentary OM. Although we did not observe significant down-core trends in the composition of OM from the selected kasten cores analyzed, there were marked contrasts among the subsurface deposits from different sites. All of these differences reflect contrasts in the sources and diagenetic history of OM within the Fly River delta-clinoform system. In order to better explain these differences, we examine several compositional parameters that can provide semiquantitative information on the provenance and degradative state of organic materials within the seabed. End-member compositions have been incorporated into this discussion to facilitate this goal. These end-member data come from published studies on the compositions of soils and vegetation from different regions of the drainage basin [*Bird et al.*, 1994], from analyses of sinking materials collected by sediment traps in the Gulf of Papua [*Burns et al.*, 2004] and from the analyses of fine and coarse suspended particulate OM samples (FPOM and CPOM, respectively) from the Fly and Strickland rivers [*Alin et al.*, 2007], as well as the analyses of floodplain sediments from the Strickland River [*Alin et al.*, 2007]. In the following discussion, we combine the information provided by these various compositional trends to better characterize the nature of the OM present in the sediments analyzed in this study.

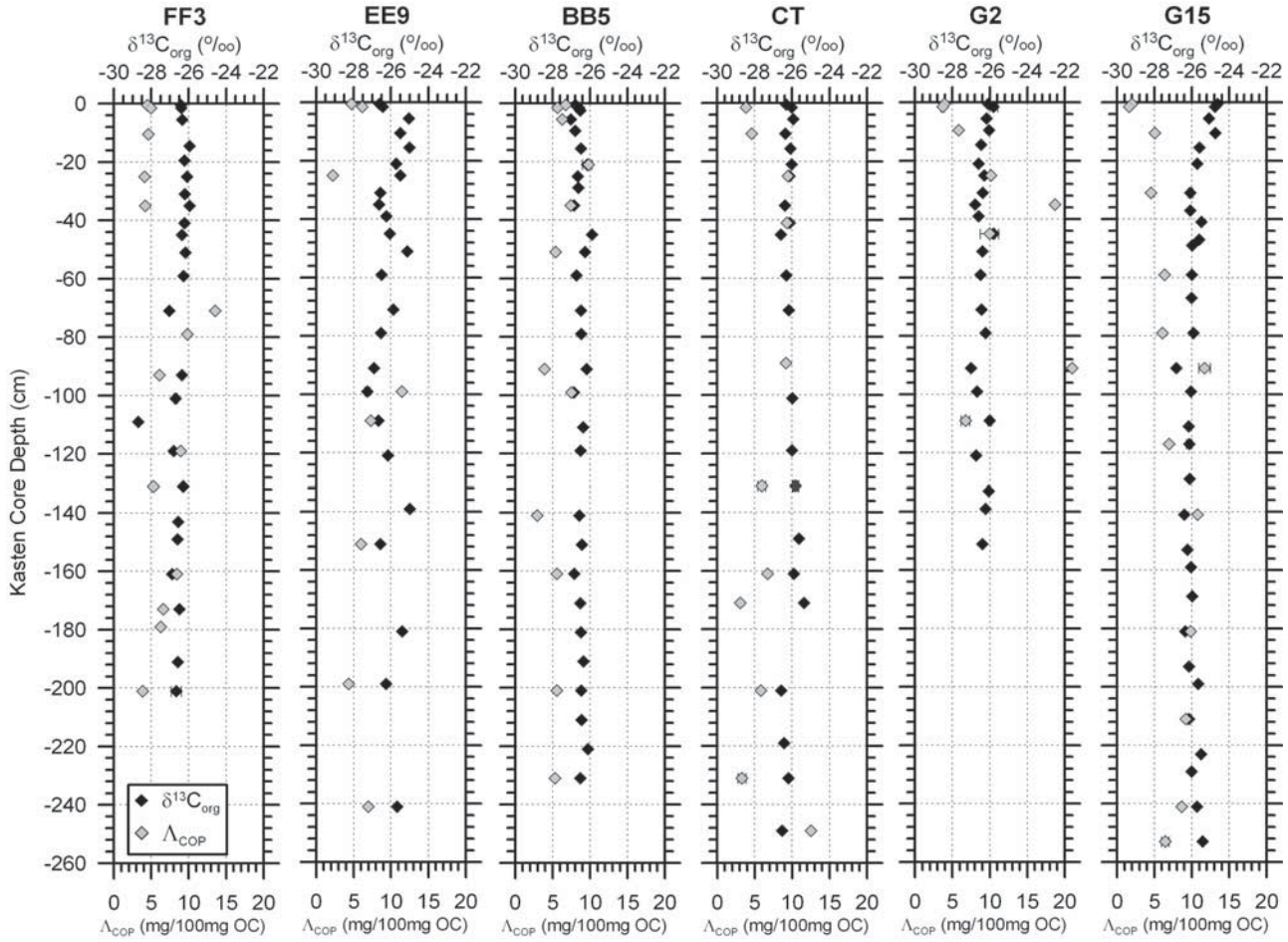

Figure 7. Down-core profiles of stable carbon compositions of organic matter ($\delta^{13}C_{org}$) and carbon-normalized yields of lignin CuO oxidation products (Λ_{COP}) from selected kasten cores.

[34] To investigate the origin of bulk OM, we plotted the $\delta^{13}C_{org}$ signatures versus the molar ON:OC ratios of all the samples analyzed (Figure 9). These graphs enable us to assess the contributions from different OM sources based on the differences of their elemental and stable carbon isotopic compositions [e.g., *Goni et al.*, 2003, 2005a]. The compositional ranges of different potential sources of OM are included in the graphs to provide a context for the seabed compositions. In Figure 9a, we plot the compositions of actual samples from the Fly/Strickland River drainage basin, including the $\delta^{13}C_{org}$ ranges of soil organic matter (SOM) determined by *Bird et al.* [1994]. Also plotted are the average ON:OC and $\delta^{13}C_{org}$ compositions of FPOM and CPOM samples from the Fly and Strickland rivers, as well as the compositions of sediments collected from different locations across transects through the Strickland River floodplain [*Alin et al.*, 2007]. This plot shows that elemental and stable carbon isotopic compositions of suspended particles and floodplain sediments are consistent with a mixture of sources, including C_3 plants and forest soils. It is interesting to highlight the contrasts in the $\delta^{13}C_{org}$ signatures of forest SOM from different altitudes, with distinctly enriched values exhibited by the high-altitude samples. Also notable are the elevated ON:OC values and enriched $\delta^{13}C_{org}$ compositions exhibited by the Gulf of Papua sediment trap samples, which fall within the range of "typical" marine algae.

[35] The compositions of the delta and clinoform sediment samples analyzed in this study show that in the case of surface sediments (Figure 9b), most high-SA samples plot along a compositional mixing line between typical C_3 vascular plants and several other potential sources, including SOM derived from C_3 plants and a mixture of marine and freshwater-estuarine algae. These data are consistent with the findings of *Bird et al.* [1995], who measured similarly depleted $\delta^{13}C_{org}$ compositions in surface samples from the Fly delta. It is difficult to further differentiate among possible sources with these data alone (see below), but it is clear that the low-SA samples contain a different mixture of OM sources based on their significantly enriched $\delta^{13}C_{org}$ compositions.

[36] The high-density samples plot in a region that is consistent with SOM being a predominant contributor (Figure 9c). In contrast, the low-density fractions displayed lower ON:OC ratios and more depleted $\delta^{13}C_{org}$ compositions that suggest their OM is derived from vascular plant fragments. The trends displayed by the down-core sediments from the selected sites suggest that the OM in these samples has similar origins to those in high-SA surface samples (Figure 9d). Notably, a number of samples from

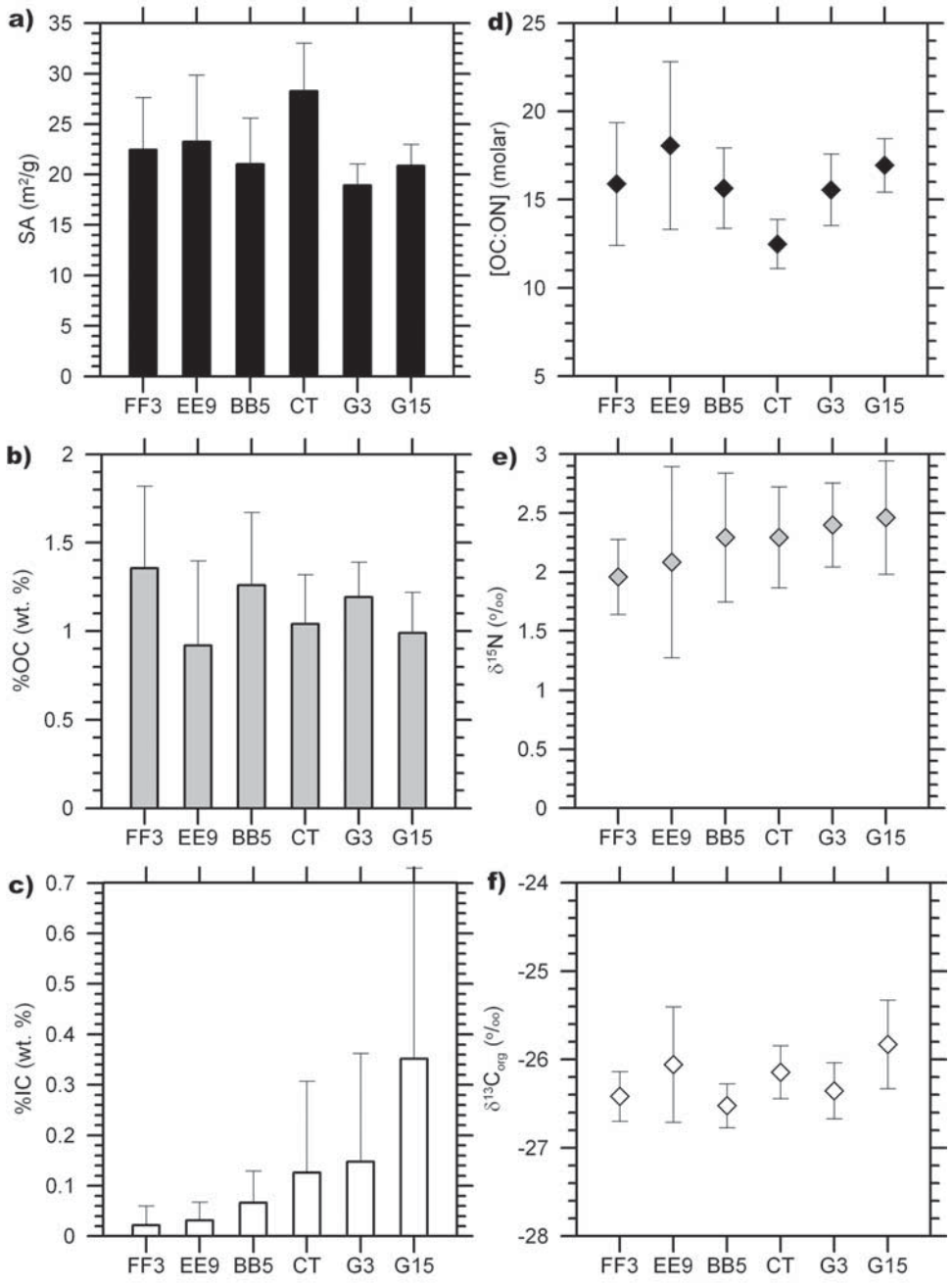

Figure 8. Average compositions of subsurface sediments from selected kasten cores. The parameters plotted include (a) mineral surface area (SA), (b) weight percent organic carbon content (%OC), (c) weight percent inorganic carbon content (%IC), (d) molar OC:ON ratios, (e) stable nitrogen isotopic compositions, and (f) stable carbon isotopic composition of organic matter ($\delta^{13}C_{org}$). Error bars indicate the variability (±1 standard error) within each site and sample type.

two sites, EE9 and G15, display slightly enriched $\delta^{13}C_{org}$ and plot toward the compositions displayed by the low-SA samples from the seabed surface (Figure 9b).

[37] A plot of $\Delta^{14}C_{org}$ versus $\delta^{13}C_{org}$ compositions provides additional insight on the nature and provenance of the different density fractions within surface sediments (Figure 10). As in the previous graphs, we have included the compositional ranges for potential end-members, including modern OM derived from vascular plant detritus, river-estuarine and marine algae. We have also included the compositional range expected for recalcitrant soil OM ($\Delta^{14}C$ of −250 to −550 ‰) with average ages ranging from 2500 to 6300 years B. P. and fossil OM (i.e., kerogen) devoid of ^{14}C ($\Delta^{14}C = -1000$ ‰). Few data are available on the composition of aged OM in Papua New Guinea. The erosion of mineral soils from steep regions of the Papua New Guinea (PNG) highlands, which are characterized by extensive gullies, may contribute to the inputs of aged OM.

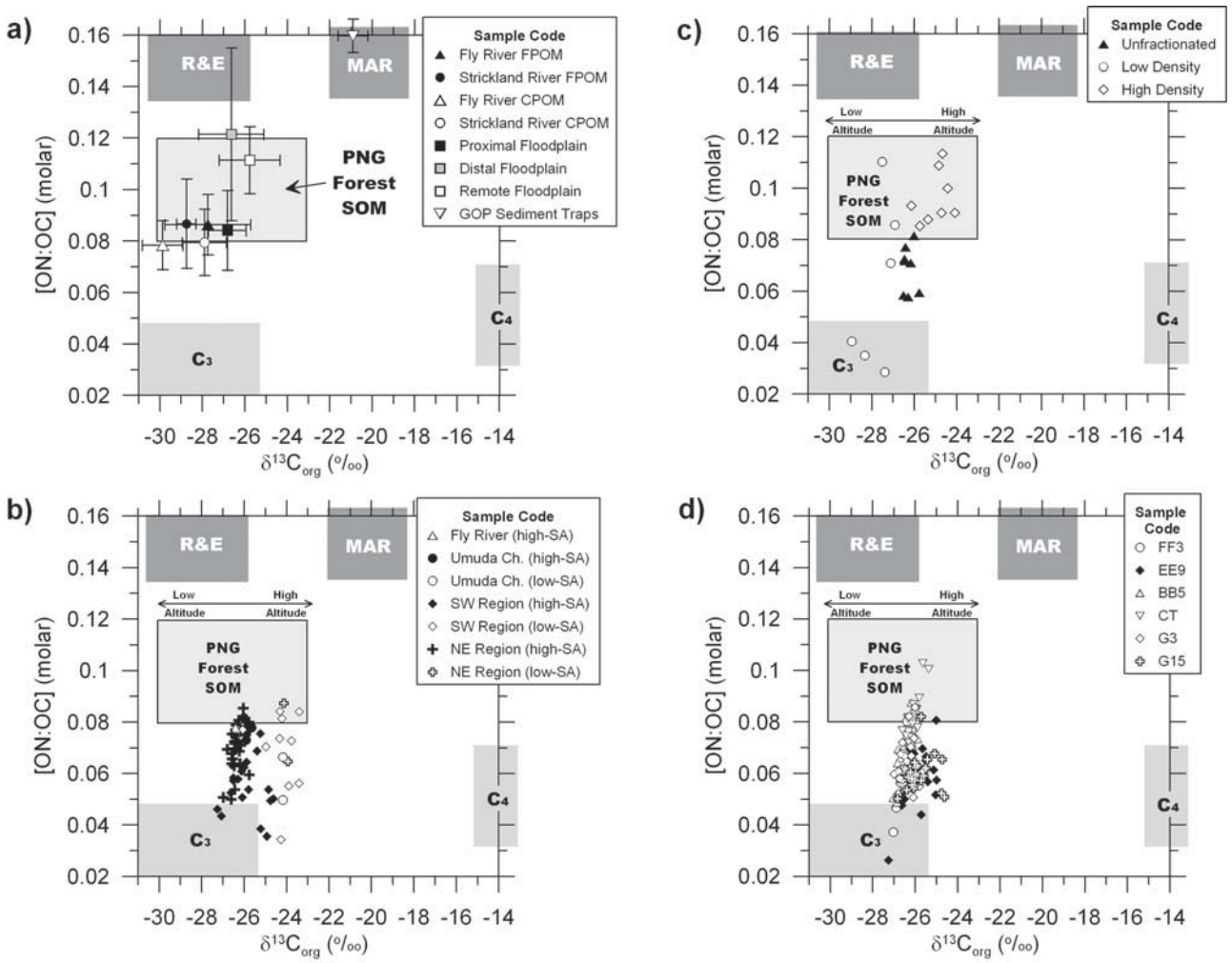

Figure 9. Relationship between stable carbon isotopic compositions ($\delta^{13}C_{org}$) and molar organic nitrogen:organic carbon ratios (ON:OC) for (a) soils, suspended river sediment, and floodplain sediments from the Fly/Strickland River watershed; (b) surface sediments of contrasting texture from different locations within the delta-clinoform system; (c) density-fractionated sediment samples; and (d) subsurface sediments from individual kasten cores. As part of Figure 9a, we have plotted the averages and standard deviations of fine particulate organic matter (FPOM < 63 μm) and coarse particulate organic matter (CPOM > 64 μm) samples collected from the Fly and Strickland rivers by *Alin et al.* [2007]. Additionally, we have included the averages and standard deviations of floodplain sediments collected at proximal (<5 m from river bank), distal (100–200 m from river bank), and remote (>250 m from river bank) locations. Detailed descriptions of these samples are provided by *Alin et al.* [2007]. Figure 9a also includes the composition of materials collected by sediment traps from sites in the open Gulf of Papua (GOP), which represent a pure marine end-member. Description of these samples is provided by *Burns et al.* [2004]. Additionally, all of these graphs show the compositional ranges of potentially important carbon sources, including C_3 vascular plants (C_3), C_4 vascular plants (C_4), riverine and estuarine algae (R&E), marine algae (MAR), and soil organic matter from Papua New Guinea forests (PNG Forest SOM). The compositional range for forest SOM is derived from the $\delta^{13}C$ compositions of soil samples from forest sites at different altitudes within PNG, which were determined by *Bird et al.* [1994]. Because N measurements were not performed as part of this study, we have assumed that the ON:OC ratios for these samples are similar to typical soils. All the other compositional ranges are based on previously published studies [*Goni et al.*, 2003, 2005a, 2005b, 2006, and references therein].

Additionally, Cenozoic and Mesozoic clastic sediments present along the southern plains [*Davies et al.*, 2005] may contribute fossil OM to the particulate load exported by the river. The predominance of metamorphic and volcanic rocks over much of the uplands of the Fly/Strickland drainage basin suggest the intensive erosion that characterizes this region of the watershed probably does not contribute to kerogen inputs because these rock types are devoid of fossil carbon. The moderate ^{14}C ages of the CPOM, FPOM and floodplain sediments samples from the Fly and Strick-

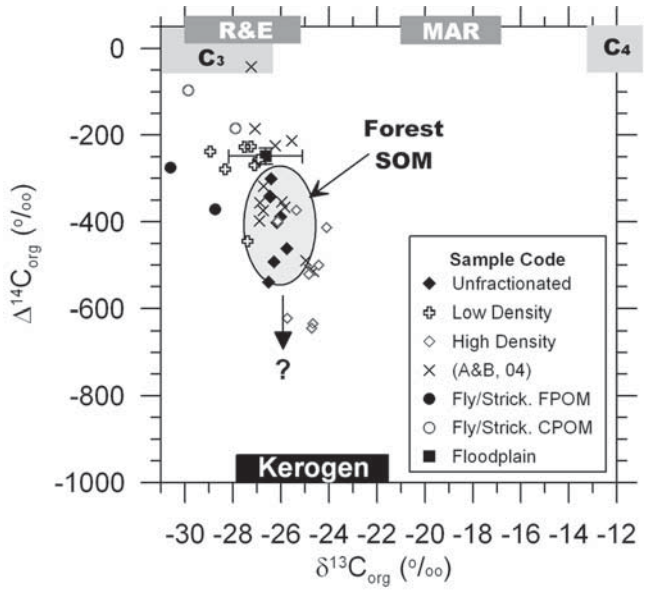

Figure 10. Relationship between stable carbon ($\delta^{13}C_{org}$) and radiocarbon isotopic ($\Delta^{14}C_{org}$) ratios for unfractionated and density-fractionated samples. For comparison, also plotted in this graph are data from unfractionated samples collected from the Fly/Strickland river watershed, including fluvial fine and coarse particulate organic matter (FPOM and CPOM, respectively) as well as floodplain sediments (see *Alin et al.* [2007] for additional details). Also included are data for bulk marine sediments from *Aller and Blair* [2004] (A&B, 04), which were derived from subsurface horizons (core depths 20–250 cm below the surface) collected along the central and western sections of the Gulf of Papua clinoform at water depths of 20–50 m. Included in these graphs are the compositional ranges of potentially important carbon sources, including C_3 vascular plants (C_3), C_4 vascular plants (C_4), riverine and estuarine algae (R&E), marine algae (MAR), C_3 forest soil organic matter (Forest SOM), and ancient kerogen (Kerogen). The compositional ranges are based on previously published studies [*Goni et al.*, 2003, 2005a, 2005b, 2006, and references therein].

land rivers, which are included in this graph (data from *Alin et al.* [2007]), may indicate the predominance of aged SOM relative to fossil kerogen inputs. Additional characterization of bedrock types, sediment sources and suspended particles from different parts of the watershed are needed to test this interpretation.

[38] Unfractionated sediments plot in a region of the graph that is consistent with the presence of aged SOM. Notably, the low-density samples plot toward the modern C_3 plant detritus, consistent with the low ON:OC ratios displayed by these samples in Figure 9b. In contrast, the high-density samples display depleted $\Delta^{14}C_{org}$ compositions that indicate their OM is of more advanced age. The $\Delta^{14}C_{org}$ compositions of most unfractionated delta-clinoform samples are slightly more depleted than those of the river POM and floodplain sediments. Several samples actually exceed the "typical" values for aged-soil OM, suggesting the presence of very old sources such as fossil kerogen. Organic matter with comparable $\delta^{13}C_{org}$ and $\Delta^{14}C_{org}$ values was detected in subsurface sediments from the Gulf of Papua clinoform (Figure 10) [*Aller and Blair*, 2004]. The presence of old terrigenous OM in surface sediments is consistent with the delivery of carbon that has been aged on land prior to its export by the Fly River. Furthermore, the slightly older ages of the sedimentary OM in delta-clinoform region relative to the fluvial POM and floodplain sediments also suggest the preferential loss of modern terrigenous carbon relative to its aged counterpart prior to deposition on the seabed. This interpretation agrees well with the results of Aller and coworkers, who measured preferential losses of modern terrigenous carbon in the inner regions of the Gulf of Papua [*Aller et al.*, 2007, and references therein].

5.1.2. Insights From CuO Oxidation Product Data

[39] The carbon-normalized yields of lignin phenols are plotted against the $\delta^{13}C_{org}$ compositions of surface and subsurface sediments to further characterize the sources of OM within the Fly River delta-clinoform system (Figure 11). Because lignin is uniquely derived from vascular land plants, the yields of lignin-derived CuO products provide a good way to differentiate between terrigenous and marine OM sources. The end-member compositions illustrate these patterns (Figure 11a). For example, CPOM samples display high Λ_{COP} values and depleted $\delta^{13}C_{org}$ compositions that are consistent with elevated contributions from vascular plant detritus. In contrasts, all floodplain sediments are characterized by low Λ_{COP} values and slightly enriched $\delta^{13}C_{org}$ compositions that indicate the presence of highly degraded lignin. Among the floodplain samples, those from the most distal and remote regions display the lowest Λ_{COP} values, most likely as a result of enhanced degradation (see *Alin et al.* [2007] for detailed discussion of river and floodplain OM compositions). In contrast, both algal OM and kerogen, the latter of which has undergone thermal alteration during the maturation of sedimentary rocks, do not contain lignin. Hence these end-members plot along the x axis at zero Λ_{COP} values (see Figure 11).

[40] All of the high-SA samples from surface sediments are characterized by depleted $\delta^{13}C_{org}$ values and intermediate Λ_{COP} values that are consistent with mixed contributions from vascular plant detritus and SOM (Figure 11b). The same can be said for virtually all of the subsurface sediments from the selected sites (Figure 11c). These results are consistent with previous studies [e.g., *Robertson and Alongi*, 1995], which identified significant contributions of mangrove-derived detritus from the Fly delta. In contrast, slightly enriched $\delta^{13}C_{org}$ signatures and very low lignin yields characterize the low-SA samples collected from the surface of the seabed. These compositions could be interpreted as contributions from a modern mixture of riverine/estuarine and marine algae, or as indication of contributions from highly altered SOM and/or ancient kerogen. On the basis of the advanced ages of the high-density fractions of surface samples (Figure 10), which we expect would be present in the coarser (low SA), we speculate that this latter possibility is the more likely explanation for the observed patterns.

[41] In order to further constrain the contributions from marine OM, we plotted the $\delta^{13}C_{org}$ versus the $\delta^{15}N$ signatures of different sample types (Figure 12). In these graphs, C_3 terrigenous sources are differentiated from marine sour-

ces by their relatively depleted $\delta^{13}C_{org}$ and $\delta^{15}N$ compositions. Figure 12a illustrates the slight variability in the signatures of FPOM, CPOM and floodplain sediments [*Alin et al.*, 2007] and their marked contrast relative to the sediment trap samples from the Gulf of Papua [*Burns et al.*, 2004]. There is a slight enrichment on both the $\delta^{13}C_{org}$ and $\delta^{15}N$ compositions of floodplain sediments relative to those from suspended sediments, most likely as a result of subaerial microbial decomposition following their initial deposition [e.g., *Quideau et al.*, 2003; *Dijkstra et al.*, 2006; *Crow et al.*, 2006]. Most notably, irrespective of texture and/or location, both surface and subsurface sediments from the Fly River delta-clinoform system (Figures 12b and 12c) display $\delta^{15}N$ compositions (+1‰ to +3‰) similar to those of floodplain sediments (Figure 12a). All of the sedimentary OM samples plot far away from the marine OM end-member, indicating little of the nitrogen in these samples appears to be derived from marine algae, including those with low Λ_{COP} values (Figure 11b).

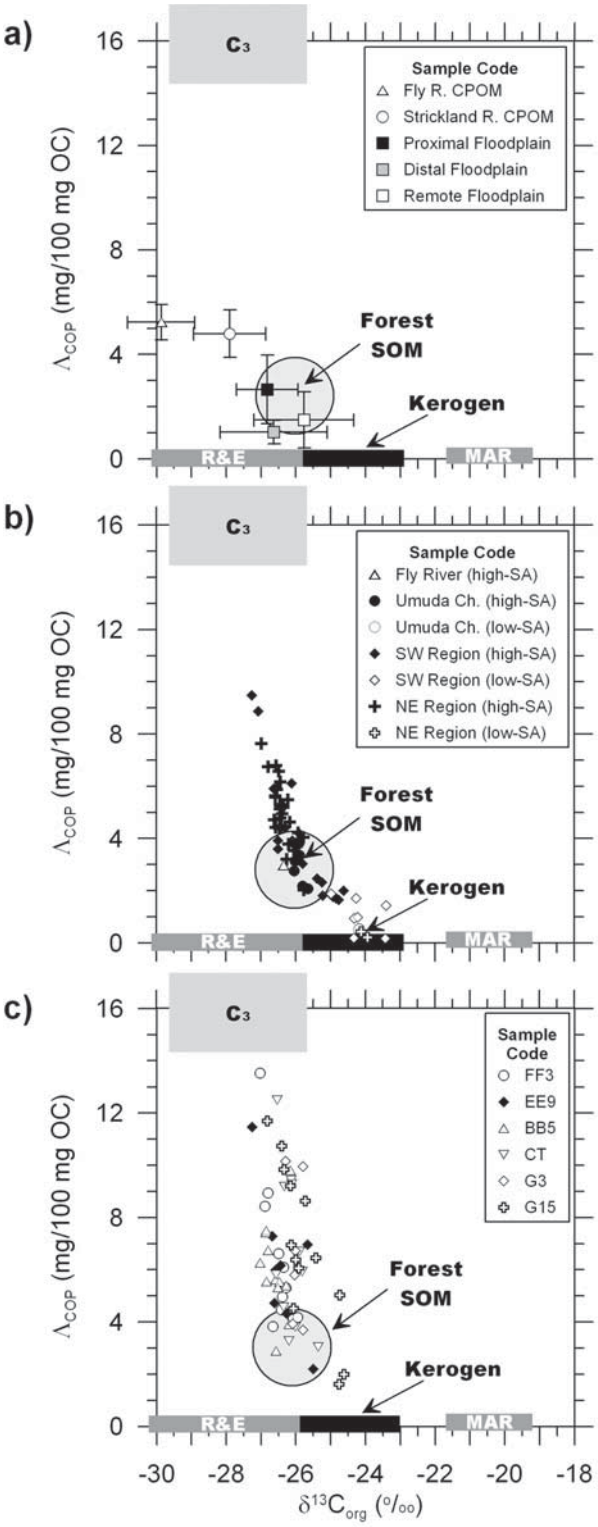

Figure 11. Relationship between carbon-normalized yields of lignin-derived CuO oxidation products (Λ_{COP}) and the stable carbon isotopic compositions of organic matter ($\delta^{13}C_{org}$) from (a) suspended river sediment and floodplain sediments from the Fly and Strickland rivers [*Alin et al.*, 2007], (b) surface sediments, and (c) subsurface sediments from individual kasten cores. Description of the different sample types is provided in the text and in previous figure captions (e.g., Figure 9). Included in these graphs are the compositional ranges of potentially important carbon sources, including C_3 vascular plants (C_3), C_4 vascular plants (C_4), riverine and estuarine algae (R&E), marine algae (MAR), C_3 forest soil organic matter (Forest SOM), and ancient kerogen (Kerogen). The compositional ranges are based on previously published studies [*Goni et al.*, 2003, 2005a, 2005b, 2006, and references therein].

[42] On the basis of these compositions (Figures 11 and 12) and the elemental ratios (Figure 9), we conclude that both surface and subsurface sediments in the Fly River delta-clinoform system predominantly contain a mixture of modern vascular plant detritus and aged SOM, with no evidence of measurable contributions from marine OM. In addition, fossil OM devoid of recognizable biochemicals may also be present, especially in the low-SA samples. These latter samples are characterized by the lowest Λ_{COP} values (Figure 11b) and plot in a region of relatively depleted $\delta^{15}N$ values and slightly enriched $\delta^{13}C_{org}$ values that is distinct from typical C_3 sources. Contributions from highly degraded SOM with a mixed C_3/C_4 source may also explain these latter compositions. At this point, additional data are needed to settle this question definitely; however, we can conclude that the coarser fraction of the sediments deposited on the delta contains a mixture of land-derived OM that is distinct from its finer counterpart.

[43] The molecular compositions of the CuO oxidation products can be summarized in ratio plots such as the ones illustrated in Figure 13 [e.g., *Goni et al.*, 2000, 2003]. In the case of S_{COP}/V_{COP} versus C_{COP}/V_{COP} ratios, the compositional ranges of different lignin-bearing sources can be superimposed on the compositions exhibited by the sedimentary OM from the study area. These graphs show that, independent of their Λ_{COP} values, both the high-SA surface samples and the subsurface samples plot in a region of elevated S_{COP}/V_{COP} ratios and relatively low C_{COP}/V_{COP} ratios. Such compositions are consistent with the lignin in these samples originating from predominantly angiosperm sources, with mixed woody and nonwoody contributions. As angiosperm tissues are degraded, it is typical to observe

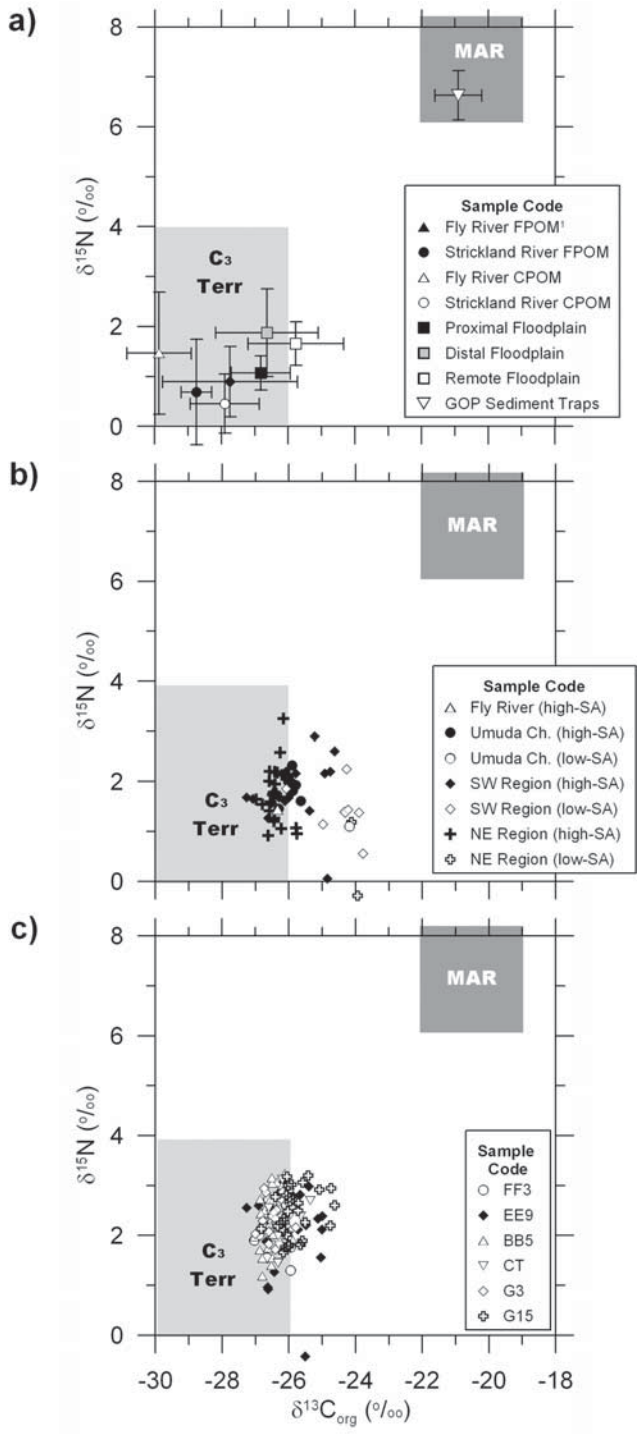

Figure 12. Relationship between stable carbon isotopic compositions ($\delta^{13}C_{org}$) and stable nitrogen isotopic compositions ($\delta^{15}N$) of OM in (a) suspended sediments and floodplain sediments from the Fly and Strickland rivers [*Alin et al.*, 2007], (b) surface sediments, and (c) subsurface sediments from kasten cores in selected locations within this system. Description of the different sample types is provided in the text and in previous figure captions (e.g., Figure 9). Included in these graphs are the compositional ranges of C_3-derived terrigenous organic matter sources and marine algal sources (based on compositional ranges summarized by *Fogel and Cifuentes* [1993]).

decreases in both their S_{COP}/V_{COP} and C_{COP}/V_{COP} ratios as syringyl and cinnamyl phenols tend to be more labile than their vanillyl counterparts [e.g., *Hedges et al.*, 1988; *Goni et al.*, 1993; *Opsahl and Benner*, 1995]. It is important to highlight the unique compositions exhibited by the low-SA samples, which were characterized by low lignin yields and enriched $\delta^{13}C_{org}$ compositions. These samples plot separately from their high-SA counterparts in Figure 13. The elevated C_{COP}/V_{COP} ratios, in particular, suggest that the lignin in these samples has a distinct origin and is most likely ultimately derived from nonwoody sources such as leaves and/or grasses. Such observations suggest that contributions from aged SOM of mixed C_3/C_4 provenance may explain the compositions exhibited by the low-SA surface sediments, as would be expected if they were derived from grasslands. Under this scenario, fossil OM may be less important than suggested by the previous discussion.

[44] Further differentiation is also observed in the plots of P_{COP}/V_{COP} versus B_{COP}/V_{COP} ratios. Both P_{COP} and B_{COP} have nonlignin precursors such as aromatic amino acids and phenolic polymers [e.g., *Goni and Hedges*, 1995]. Elevated yields of these compounds relative to lignin products have been measured in soils, where microbial biomass (i.e., bacteria, fungi) and degraded polymers are more abundant than intact lignin molecules [e.g., *Prahl et al.*, 1994; *Goni and Thomas*, 2000]. Hence we interpret the fact that the low-SA samples are characterized by high P_{COP}/V_{COP} and B_{COP}/V_{COP} ratios relative to their high-SA counterparts as an indication that the coarser deposits contain highly altered OM devoid of intact lignin. Further confirmation of this explanation is the elevated acid:aldehyde yields of low-SA samples (vanillyl acid:aldehyde ratios of 0.8 to over 1.0) relative to those measured in the high-SA samples (vanillyl acid:aldehyde ratios of 0.5 to 0.6). Because of the low yields, we were unable to measure the isotopic compositions of lignin phenols from the low-SA samples. However, their distinct CuO product ratios suggest their OM ultimately originated from a different source. We speculate that there could be a distinct source of coarse particles within the watershed that is characterized by different vegetation (e.g., grasslands) and/or diagenetic history, which impart the unique signatures observed in the delta. It is possible that the processes (e.g., winnowing, resuspension) responsible for the formation of these coarse deposits also increase the extent of degradation in the remaining OM. Thus we cannot discount the possibility that the unique compositions observed in the low-SA samples are partially due to in situ degradation. Better sampling of materials brought in by the river, including characterization of different size/density classes of the river particulate load, are needed to critically evaluate these possibilities.

5.2. Diagenetic State of OM in the Seabed

[45] After evaluating the composition and character of the OM in the sediments throughout the Fly River delta-clinoform system, it is clear that terrigenous sources are dominant in both the surface and deeper horizons of the seabed. Our data show no significant evidence for the dilution of the terrigenous OM by marine sources. In this context, an important question that remains is what fraction of the particulate OM load exported to the ocean by rivers is preserved in the sediments versus what fraction is degraded

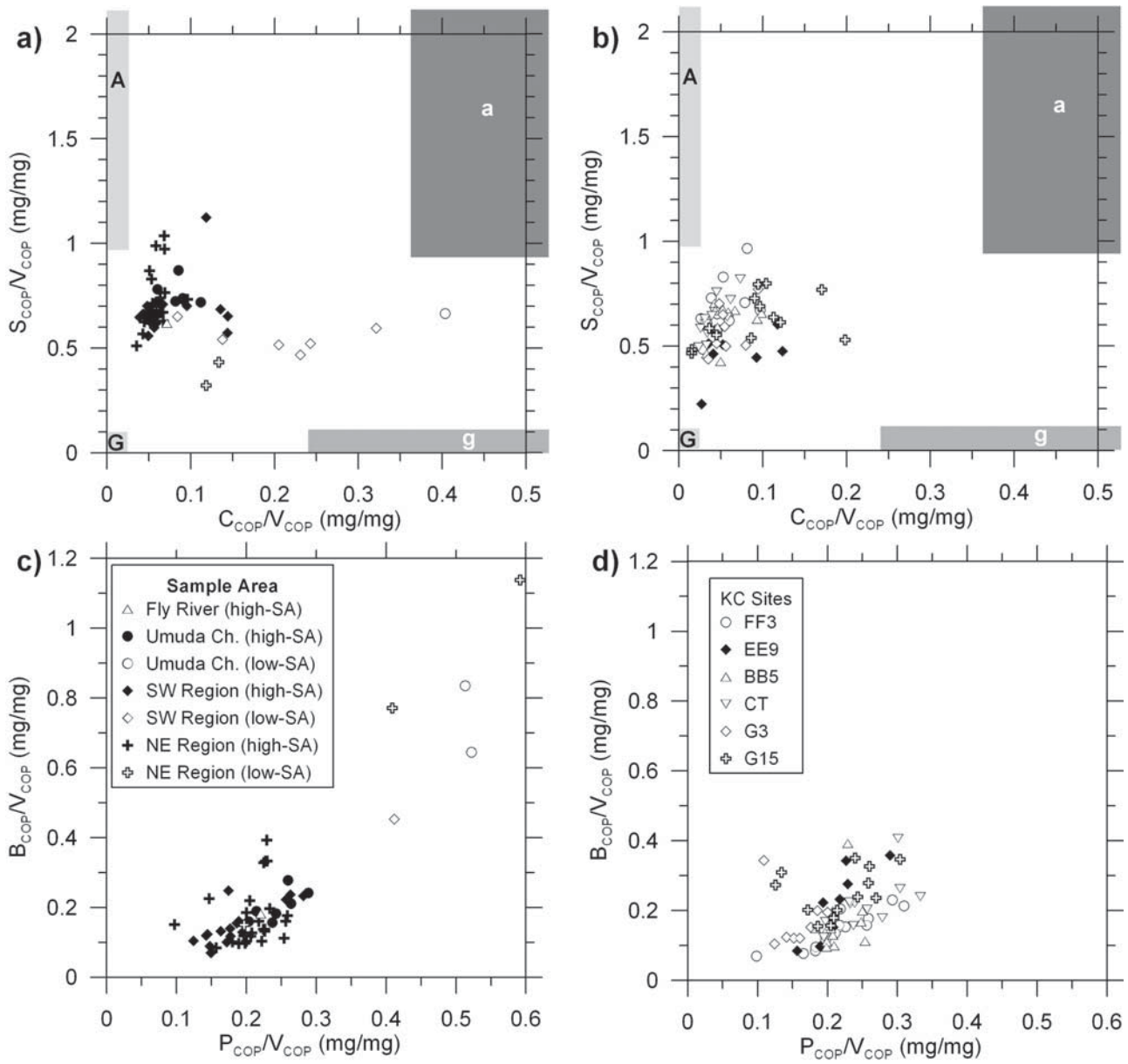

Figure 13. Compositional ratios of CuO oxidation products for surface and subsurface sediments. Plotted in these graphs are cinnamyl/vanillyl phenol ratios (C_{COP}/V_{COP}) versus syringyl/vanillyl phenol ratios (S_{COP}/V_{COP}) for (a) surface sediments and (b) subsurface sediments from individual kasten cores, as well as *p*-hydroxybenzoic acids/vanillyl ratios (P_{COP}/V_{COP}) versus benzoic acids/vanillyl phenol ratios (B_{COP}/V_{COP}) for (c) surface and (d) subsurface sediments. Description of the different sample types is provided in the text and in previous figure captions (e.g., Figure 9). The sample code for surface samples (Figures 13a and 13c) is plotted in Figure 13c, whereas the sample code for subsurface samples (Figures 13b and 13d) is plotted in Figure 13d. Included in these graphs are the compositional ranges of potentially important lignin sources, including gymnosperm woods (G), gymnosperm needles (g), angiosperm woods (A), and angiosperm leaves (a). The compositional ranges are based on previously published studies [*Goni et al.*, 2000, 2003, and references therein].

by microbial activity in the nearshore region [e.g., *Aller et al.*, 2004; *McKinnon et al.*, 2007]. One way to answer this question is to build a detailed OM budget for the region. At this point, we do not have enough information regarding the river fluxes and burial rates throughout the clinoform region to accurately constrain OM fluxes. However, an alternative approach to assess the degree of sedimentary OM preservation is to use the relationship between %OC content and mineral surface area [e.g., *Mayer*, 1994; *Keil et al.*, 1994; *Hedges and Keil*, 1995; *Goni et al.*, 2005b]. For example, the preferential degradation of terrigenous OM in the study area would result in depleted OC contents relative to the mineral surface area, leading to carbon loadings (i.e.,

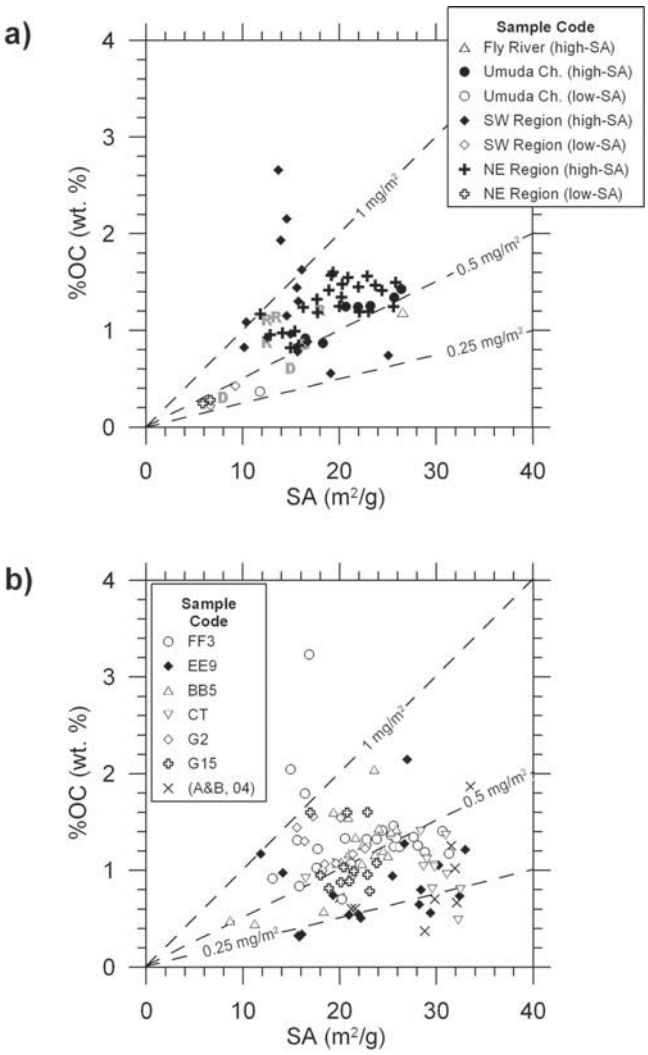

Figure 14. Relationship between mineral surface area (SA) and organic carbon content (%OC) for (a) surface and (b) subsurface sediments. Included in these graphs are lines identifying different levels of carbon loadings, including OC:SA ratios of 1.0, 0.5, and 0.25 mg C m^{-2} sediment. Description of the different sample types is provided in the text and in previous figure captions (e.g., Figure 9). Values for "typical" shelf sediments range between 0.5 and 1.0 mg C m^{-2}, while lower values indicate enhanced OC losses [*Mayer*, 1994; *Keil et al.*, 1997]. Included in Figure 13a are data from *Keil et al.* [1997], including suspended particles from the Fly River (R) and surface sediments from the Fly delta (D). Included in Figure 13b are data from *Aller and Blair* [2004] (A&B, 04), which were derived from subsurface samples (core depths 20–250 cm below the surface) collected along the central and western sections of the Gulf of Papua clinoform at water depths of 20–50 m.

OC:SA) that are lower than those measured in "normal" shelf environments [e.g., *Keil et al.*, 1997].

[46] Figure 14 illustrates the relationship between %OC and SA in both surface and subsurface sediments. For comparison, data from river and delta samples previously measured by *Keil et al.* [1997] and from clinoform samples analyzed by *Aller and Blair* [2004] are also included in these graphs. Among the surface sediments, there is a general positive relationship between %OC and SA, consistent with the control that mineral surfaces have on the stabilization of OC levels through sorption [*Mayer*, 1994; *Keil et al.*, 1994]. However, it is important to note that in two of the regions (NE and SW), the relationship between %OC and SA is not statistically significant ($r^2 = 0.22$, $p = 0.12$; $r^2 = 0.07$, $p = 0.5$, respectively). Hence other factors besides simple mineral surface area affect the %OC levels of these deposits. Nevertheless, virtually all of the high-SA samples plot in a region delineated between OC:SA ratios of 0.5 and 1.0 mg C m^{-2} (Figure 14a). These OC:SA ratios are typical of normal surface sediments in continental shelves (i.e., "monolayer-equivalent" levels) [*Mayer*, 1994]. Because these samples predominantly contain terrigenous OM (see previous discussion), it appears that along the Fly River delta-clinoform system, most of the land-derived OC is deposited on the seabed without the intense degradative losses that have been documented in other deltaic systems (e.g., OC:SA ratios from 0.25 to 0.5 mg m^{-2}) [*Keil et al.*, 1997].

[47] A few samples from the SW region plot above the 1.0 mg C m^{-2} line, indicating higher than normal OC contents, most likely due to large contributions from vascular plant detritus. On the other hand, all of the low-SA samples (and a couple of high-SA samples from the SW) plot below 0.5 mg C m^{-2} line, suggesting these samples have "submonolayer" carbon levels. These are the only samples that agree well with previously published data [*Keil et al.*, 1997]; suggesting prior studies may have missed the compositional heterogeneity of the Fly River delta-clinoform system. It is possible that the low OC:SA ratios are a result of enhanced degradation associated with coarser deposits (e.g., resuspension, winnowing). Alternatively, the distinct provenance that characterizes low-SA samples (see previous discussion) may also impart characteristically low OC loadings. Hence the low OC:SA ratios of these samples could reflect processes in the drainage basin, rather than degradative processes with the delta-clinoform system. A comprehensive characterization of the composition and provenance of the river suspended load is needed to differentiate among these hypotheses.

[48] The relationship between %OC and SA in subsurface sediments also displays large variability, both among sites but also within each of the cores (Figure 14b). In most sites, the relationship between %OC and SA was not significant ($r^2 < 0.15$; $P > 0.1$). Only the sediments from BB5 displayed as statistically significant relationship between these two variables ($r^2 = 0.5$; $P = 0.001$). As was the case for surface samples, this means that other factors besides simple mineral surface area contribute to the OC levels in the subsurface sediments. A large number of samples from the kasten cores plot within the "monolayer-equivalent" levels (0.5 to 1.0 mg C m^{-2}). Notably, a significant number of samples from some sites, such as CT, G15 and EE9, display low OC:SA ratios (0.25 to 0.5 mg C m^{-2}). These samples are consistent with the compositions determined by *Aller and Blair* [2004], who measured %OC and SA values of subsurface sediments from the central and eastern part of the Gulf of Papua. Despite the caveats associated with provenance, these "submonolayer-equivalent" OC levels can be interpreted to indicate that OM in these sediments has

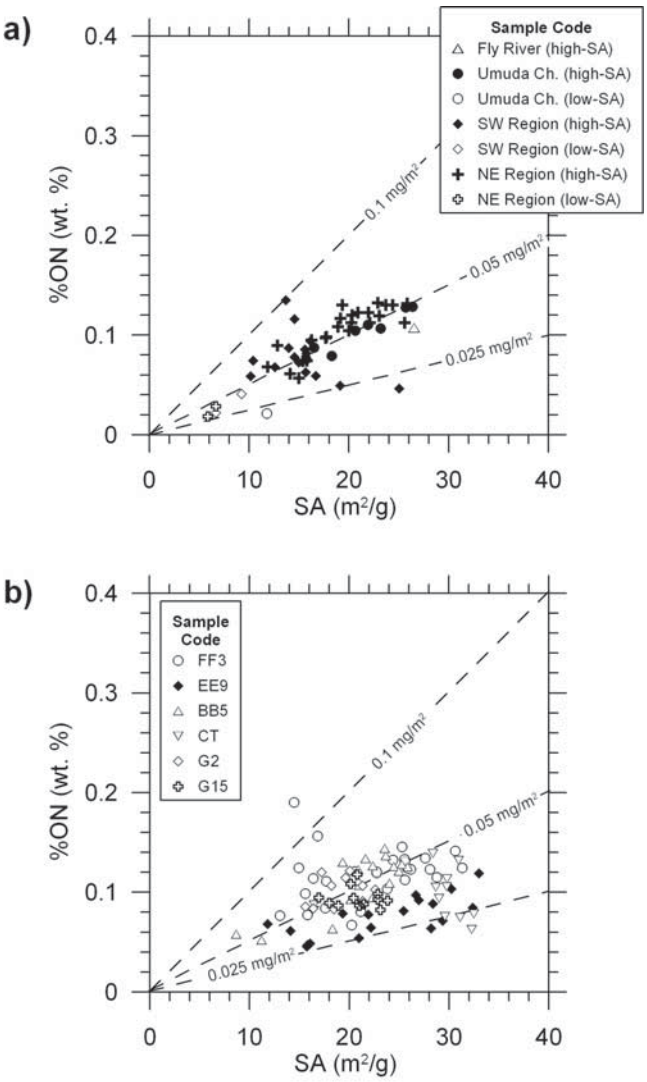

Figure 15. Relationship between mineral surface area (SA) and organic nitrogen content (%ON) for (a) surface and (b) subsurface sediments. Included in these graphs are lines identifying different levels of nitrogen loadings, including ON:SA ratios of 0.1, 0.05, and 0.025 mg ON m^{-2} sediment. Description of the different sample types is provided in the text and in previous figure captions (e.g., Figure 9). Values for "typical" shelf sediments range between 0.01 and 0.05 mg ON m^{-2} sediment, while lower values indicate enhanced ON losses [e.g., *Mayer et al.*, 1998].

undergone a significant amount of degradation. Some of the sites with low OC:SA ratios correspond to areas of negligible sediment accumulation (e.g. EE9, G15), so it is likely that the enhanced levels of degradation reflect the lack of input of fresh materials to the sediment column. We conclude that the areas of sediment bypass within the Fly River delta-clinoform system [e.g., *Martin et al.*, 2007] are likely to be the areas where OM degradation is most intense.

[49] Several of the samples from the EE9 and G15 kasten cores that display the low OC:SA ratios are characterized by slightly enriched $\delta^{13}C_{org}$ compositions and low Λ_{COP} values (e.g., Figures 9c and 11c). All of these trends are consistent with higher relative contributions from SOM, which may have resulted from the degradation of the more labile vascular plant detritus. Hence the down-core data from these sites support the idea that under conditions of low sediment accumulation and energetic physical reworking, the more labile fractions of terrigenous OM (e.g., vascular plant detritus) within the seabed are preferentially degraded, leaving behind deposits enriched in the more recalcitrant SOM (and/or kerogen) and characterized by relatively low OC:SA ratios. This interpretation is consistent with the conclusions of *Aller and Blair* [2004], who investigated carbon diagenesis in sediment cores located east of our study site (Figure 14b).

[50] Plots of SA versus %ON contents (Figure 15) illustrate a similar pattern to that observed for %OC. While there is significant variability from region to region, most high-SA surface sediments plot along a general positive relationship between %ON and SA, with a slope of ~0.05 mg m^{-2} (Figure 15a). However, there are several samples that display higher (up to 0.1 mg m^{-2}) and lower ON:SA ratios (~0.025 mg m^{-2}). As was the case for OC loadings, the low-SA samples display the lowest ON:SA ratios. In the case of subsurface sediments, there is large variability in the relationship between %ON and SA within and among cores (Figure 15b). Overall, however, most samples plot along the 0.05 mg m^{-2}, with samples from sites with negligible accumulation rates, such as EE9, plotting along a lower slope (0.025 mg m^{-2}). The N-loading levels measured in most of the sediments (ON:SA ratios of 0.05–0.025 mg m^{-2}) are comparable to those from other river-dominated margins [e.g., *Mayer et al.*, 1998] and consistent with a moderate degree of degradation. In contrast, the low N loadings (ON:SA < 0.025 mg m^{-2}) indicative of extensive degradation are consistently observed in sites from sediment bypass regions (such as EE9). Notably, the OC:SA and ON:SA ratios were highly correlated in both surface and subsurface samples ($r^2 = 0.7$), suggesting both OC and ON have similar overall reactivity in this system.

6. Summary

[51] Terrigenous OM is the predominant component of the organic carbon present in surface and subsurface sediments of the Fly River delta-clinoform system. The major sources of this land-derived OM are C_3 vegetation and C_3 soil OM, the latter of relatively advanced age. There is no evidence for the addition of marine OM and its incorporation into the sedimentary matrix. The lack of marine carbon and the low concentration of vascular plant detritus throughout most of the delta-clinoform system are consistent with the removal of the more labile components of the OM [e.g., *Aller et al.*, 2007]. However, only a few sites within the sediment bypass region of the topset appear to contain the OC-depleted sediments that typify the incineration zones found in the some of the inner regions of river margins [e.g., *Aller et al.*, 2004, 2007]. The spatial and down-core contrasts in OM concentration and composition suggest sediment transport processes are critical in determining the ultimate composition of the organic materials sequestered in these sediments. Clearly, the heterogeneous depositional environments encountered in this river-dominated margin play a key role in shaping the organic geochemistry of its

sediments and our ability to understand the processes responsible for the observed patterns.

[52] Overall, the findings of this study indicate tropical, mountainous river margins can sequester significant amounts of carbon over decadal to century timescales. Most of it appears to be terrigenous in origin and derived from recalcitrant sources such as aged soil OM. The contrast between the temporal scales of burial and the age of sedimentary OM, which is salient feature of this and many other river-dominated margins, has significant implications for the global carbon of cycle that warrant further exploration. Most of the terrigenous OM actively deposited within the Fly River delta-clinoform system experiences some depositional alteration, but its overall extent is much less than implied by previous studies [e.g., *Keil et al.*, 1997]. The areas where there appears to be extensive losses of terrigenous carbon are restricted to sediment bypass regions, characterized by low net sediment accumulation and energetic physical reworking [e.g., *Aller et al.*, 2004, 2007]. In most other areas of the Fly River delta-clinoform system, the OC loadings are consistent with relatively efficient sequestration. We conclude that the physical processes (e.g., river discharge, tides, waves), which to a large degree control the transport and deposition of particles in this and other river-dominated margins, exert a dominant role in determining the ultimate fate of particle-bound organic materials exported from land.

[53] **Acknowledgments.** Sampling of the Fly River delta was made possible by the R/V *Western Venturer* and her crew and the Ok Tedi Mining Company and Jim Veness (Ok Tedi) and was facilitated by Jim Robins (PNG National Research Institute). Wayne McCool, David Shelley, Joel Rowland, Debbie Nittrouer, and Marie Bera provided invaluable help in the field. Hugh Davies and Sioni Sioni of the University of Papua New Guinea facilitated our work in PNG. Zou Zou Kuzyk helped with the CuO oxidation analyses of the river samples. This research was supported by funds from the National Science Foundation through the Chemical Oceanography (OCE-0220600 grant to M. Goni) and MARGINS Programs (OCE-0203351 and OCE-0504616 to C. Nittrouer and A. Ogston). Radiocarbon analyses were performed through the auspices of the U.S. Department of Energy by the University of California/Lawrence Livermore National Laboratory under contract W-7405-Eng-48. Funding for the radiocarbon analyses was provided to T. Guilderson by UC/LLNL 04-ERD-060. This manuscript benefited from comments and input from Bob Aller, Hugh Davies, and one anonymous reviewer.

References

Aalto, R., J. W. Lauer, and W. E. Dietrich (2007), Spatial and temporal dynamics of sediment accumulation and exchange along Strickland River floodplains (Papua New Guinea) over decadal-to-centennial timescales, *J. Geophys. Res.*, doi:10.1029/2006JF000627, in press.

Alexander, C. R., D. J. DeMaster, and C. A. Nittrouer (1991), Sediment accumulation in a modern epicontinental-shelf setting: The Yellow Sea, *Mar. Geol.*, *98*, 51–72.

Alin, S. R., R. Aalto, M. A. Goni, J. E. Richey, and W. E. Dietrich (2007), Biogeochemical characterization of carbon sources in the Strickland and Fly rivers, Papua New Guinea, *J. Geophys. Res.*, doi:10.1029/2006JF000625, in press.

Aller, J. Y., and R. C. Aller (2004), Physical disturbance creates bacterial dominance of benthic biological communities in tropical deltaic environments of the Gulf of Papua, *Cont. Shelf Res.*, *24*, 2395–2416.

Aller, R. C. (2001), Transport and reactions in the bioirrigated zone, in *The Benthic Boundary Layer*, edited by B. P. Boudreau and B. B. Jorgensen, pp. 269–301, Oxford Univ. Press, New York.

Aller, R. C., and N. E. Blair (2004), Early diagenetic remineralization of sedimentary organic C in the Gulf of Papua deltaic complex (Papua New Guinea): Net loss of terrestrial C and diagenetic fractionation of C isotopes, *Geochim. Cosmochim. Acta*, *68*, 1815–1825.

Aller, R. C., A. Hannides, C. Heilbrun, and C. Panzeca (2004), Coupling of early diagenetic processes and sedimentary dynamics in tropical shelf environments: The Gulf of Papua deltaic complex, *Cont. Shelf Res.*, *24*, 2455–2486.

Aller, R. C., N. E. Blair, and G. J. Brunskill (2007), Early diagenetic cycling, incineration, and burial or sedimentary organic carbon in the central Gulf of Papua (Papua New Guinea), *J. Geophys. Res.*, doi:10.1029/2006JF000689, in press.

Alongi, D. M. (1995), Decomposition and recycling of organic matter in muds of the Gulf of Papua, northern Coral Sea, *Cont. Shelf Res.*, *15*, 1319–1337.

Alongi, D. M., P. Christoffersen, F. Tirendi, and A. I. Robertson (1992), The influence of freshwater and material export on sedimentary facies and benthic processes within the Fly delta and adjacent Gulf of Papua (Papua New Guinea), *Cont. Shelf Res.*, *12*, 287–326.

Ayukai, T., and E. Wolanksi (1997), Importance of biologically mediated removal of fine sediments from the Fly River Plume, Papua New Guinea, *Estuarine Coastal Shelf Sci.*, *44*, 629–639.

Bain, J. H. C., H. L. Davies, P. D. Hohnen, R. J. Ryburn, I. E. Smith, R. Grainger, R. J. Tingey, and M. R. Moffat (1973), Geological map of Papua New Guinea 1:1,000,000 scale, Bur. of Miner. Resour., Canberra.

Benner, R., and S. Opsahl (2001), Molecular indicators of the sources and transformations of dissolved organic matter in the Mississippi river plume, *Org. Geochem.*, *32*(4), 597–611.

Berner, R. A. (1982), Burial of organic carbon and pyrite sulfur in the modern ocean: Its geochemical and environmental significance, *Am. J. Sci.*, *282*, 451–473.

Bird, M. I., S. G. Haberle, and A. R. Chivas (1994), Effect of altitude on the carbon-isotope composition of forest and grassland soils from Papua New Guinea, *Global Biogeochem. Cycles*, *8*, 13–22.

Bird, M. I., G. J. Brunskill, and A. R. Chivas (1995), Carbon isotope composition of sediments from the Gulf of Papua, *Geo Mar. Lett.*, *15*, 153–159.

Blair, N. E., E. L. Leithold, and R. C. Aller (2004), From bedrock to burial: The evolution of particulate organic carbon across coupled watershed-continental margin systems, *Mar. Chem.*, *92*, 141–156.

Bock, M. J., and L. M. Mayer (2000), Mesodensity organo-clay associations in a near-shore sediment, *Mar. Geol.*, *163*, 65–75.

Brunskill, G. J. (2004), New Guinea and its coastal seas, a testable model of wet tropical coastal processes: An introduction to Project TROPICS, *Cont. Shelf Res.*, *24*, 2273–2295.

Burns, K. A., P. Greenwood, R. Benner, D. Brinkman, G. Brunskill, S. Codi, and I. Zagorskis (2004), Organic biomarkers for tracing carbon cycling in the Gulf of Papua (Papua New Guinea), *Cont. Shelf Res.*, *24*, 2373–2394.

Christie-Blick, N., and N. W. Driscoll (1995), Sequence stratigraphy, *Annu. Rev. Earth Planet. Sci.*, *23*, 451–478.

Crockett, J. S. (2006), Unraveling the three-dimensional characteristics of clinoforms: Gulf of Papua, New Guinea, Ph.D. thesis, Univ. of Wash., Seattle.

Crockett, J. S., C. A. Nittrouer, A. S. Ogston, and M. A. Goñi (2008), Variable styles of sediment accumulation impacting strata formation on a clinoform: Gulf of Papua, Papua New Guinea, in *The Fly River System—Papua New Guinea: Natural and Human Aspects of a Complex Fluvial System, Dev. Earth Environ. Sci.*, vol. 9, edited by B. R. Bolton, Elsevier, New York, in press.

Crow, S. E., E. W. Sulzman, W. D. Rugh, R. D. Bowden, and K. Lajtha (2006), Isotopic analysis of respired CO_2 during decomposition of separated soil organic matter pools, *Soil Biol. Biochem.*, *38*, 3279–3291.

Davies, H. L., P. Bani, P. M. Black, E. Garaebiti, P. Rodda, and I. E. Smith (2005), Geology of Oceania (including Fiji, PNG and Solomons), in *Encyclopedia of Geology*, vol. 4, edited by R. Selley et al., pp. 109–123, Elsevier, New York.

Davies, P. (2004), Nutrient processes and chlorophyll in the estuaries and plume of the Gulf of Papua, *Cont. Shelf Res.*, *24*, 2317–2341.

Dietrich, W. E., G. Day, and G. Parker (1999), The Fly River, Papua New Guinea: Inferences about river dynamics, floodplain sedimentation and fate of sediment, in *Varieties of Fluvial Form*, edited by A. J. Miller and A. Gupta, pp. 345–376, John Wiley, Hoboken, N. J.

Dijkstra, P., A. Ishizu, R. Doucett, S. C. Hart, E. Schwartz, O. V. Menyailo, and B. A. Hungate (2006), ^{13}C and ^{15}N natural abundance of the soil microbial biomass, *Soil Biol. Biochem.*, *38*, 3257–3266.

Fogel, M. L., and L. A. Cifuentes (1993), Isotope fractionation during primary production, in *Organic Geochemistry*, edited by M. H. Engel and S. A. Macko, pp. 73–98, Springer, New York.

Goni, M. A., and T. I. Eglinton (1996), Stable carbon isotopic analyses of lignin-derived CuO oxidation products by isotope ratio monitoring-gas chromatography-mass spectrometry (irm-GC-MS), *Org. Geochem.*, *24*, 601–615.

Goni, M. A., and J. I. Hedges (1995), Sources and reactivities of marine-derived organic matter in coastal sediments as determined by alkaline CuO oxidation, *Geochim. Cosmochim. Acta*, *59*, 2965–2981.

Goni, M. A., and S. Montgomery (2000), Alkaline CuO oxidation with a microwave digestion system: Lignin analyses of geochemical samples, *Anal. Chem.*, *72*, 3116–3121.

Goni, M. A., and K. A. Thomas (2000), Sources and transformations of organic matter in surface soils and sediments from a tidal estuary (north inlet, South Carolina, USA), *Estuaries*, *23*, 548–564.

Goni, M. A., B. Nelson, R. A. Blanchette, and J. I. Hedges (1993), Fungal degradation of wood lignins: Geochemical perspectives from CuO-derived phenolic dimers and monomers, *Geochim. Cosmochim. Acta*, *57*, 3985–4002.

Goni, M. A., M. B. Yunker, R. W. Macdonald, and T. I. Eglinton (2000), Distribution and sources of organic biomarkers in Arctic sediments from the Mackenzie River and Beaufort shelf, *Mar. Chem.*, *71*, 23–51.

Goni, M. A., M. J. Teixeira, and D. W. Perkey (2003), Sources and distribution of organic matter in a river-dominated estuary (Winyah Bay, SC, USA), *Estuarine Coastal Shelf Sci.*, *57*, 1023–1048.

Goni, M. A., M. W. Cathey, Y. H. Kim, and G. Voulgaris (2005a), Fluxes and sources of suspended organic matter in an estuarine turbidity maximum region during low discharge conditions, *Estuarine Coastal Shelf Sci.*, *63*, 683–700.

Goni, M. A., M. B. Yunker, R. W. Macdonald, and T. I. Eglinton (2005b), The supply and preservation of ancient and modern components of organic carbon in the Canadian Beaufort Shelf of the Arctic Ocean, *Mar. Chem.*, *93*, 53–73.

Goni, M. A., N. Monacci, R. Gisewhite, A. Ogston, J. Crockett, and C. Nittrouer (2006), Distribution and sources of particulate organic matter in the water column and sediments of the Fly River delta, Gulf of Papua (Papua New Guinea), *Estuarine Coastal Shelf Sci.*, *69*, 225–245.

Gordon, E. S., and M. A. Goni (2003), Sources and distribution of terrigenous organic matter delivered by the Atchafalaya River to sediments in the northern Gulf of Mexico, *Geochim. Cosmochim. Acta*, *67*, 2359–2375.

Gordon, E. S., and M. A. Goni (2004), Controls on the distribution and accumulation of terrigenous organic matter in sediments from the Mississippi and Atchafalaya River margin, *Mar. Chem.*, *92*, 331–352.

Gordon, E. S., M. A. Goni, Q. N. Roberts, G. C. Kineke, and M. A. Allison (2001), Organic matter distribution and accumulation on the inner Louisiana shelf west of the Atchafalaya River, *Cont. Shelf Res.*, *21*, 1691–1721.

Harris, P. T., E. K. Baker, A. R. Cole, and S. A. Short (1993), A preliminary study of sedimentation in the tidally dominated Fly River delta, Gulf of Papua, *Cont. Shelf Res.*, *13*, 441–472.

Harris, P. T., M. G. Hughes, E. K. Baker, R. W. Dalrymple, and J. B. Keene (2004), Sediment transport in distributary channels and its export to the pro-deltaic environment in a tidally dominated delta: Fly River, Papua New Guinea, *Cont. Shelf Res.*, *24*, 2431–2454.

Hedges, J. I., and R. G. Keil (1995), Sedimentary organic matter preservation: An assessment and speculative synthesis, *Mar. Chem.*, *49*, 81–115.

Hedges, J. I., W. A. Clark, P. D. Quay, J. E. Richey, A. H. Devol, and U. M. Santos (1986), Compositions and fluxes of particulate organic material in the Amazon River, *Limnol. Oceanogr.*, *31*, 717–738.

Hedges, J. I., R. A. Blanchette, K. Weliky, and A. H. Devol (1988), Effects of fungal degradation on the CuO oxidation products of lignin: A controlled laboratory study, *Geochim. Cosmochim. Acta*, *52*, 2717–2726.

Keil, R. G., E. Tsamakis, C. B. Fuh, J. C. Giddings, and J. I. Hedges (1994), Mineralogical and textural controls on the organic composition of coastal marine sediments: Hydrodynamic separation using SPLITT-fractionation, *Geochim. Cosmochim. Acta*, *58*, 879–893.

Keil, R. G., L. M. Mayer, P. D. Quay, J. E. Richey, and J. I. Hedges (1997), Loss of organic matter from riverine particles in deltas, *Geochim. Cosmochim. Acta*, *61*, 1507–1511.

Korner, C., G. D. Farquhar, and Z. Roksandic (1988), A global survey of carbon isotope discrimination in plants from high altitude, *Oecologia*, *74*, 623–632.

Korner, C., G. D. Farquhar, and S. C. Wong (1991), Carbon isotope discrimination follows latitudinal and altitudinal trends, *Oecologia*, *88*, 30–40.

Kuehl, S. A., C. A. Nittrouer, and D. J. DeMaster (1986), Distribution of sedimentary structures in the Amazon subaqueous delta, *Cont. Shelf Res.*, *6*, 311–336.

Kuehl, S. A., T. M. Hariu, and W. S. Moore (1989), Shelf sedimentation off the Ganges–Brahmaputra river system: Evidence for sediment bypassing to the Bengal fan, *Geology*, *17*, 1132–1135.

Leithold, E., and N. Blair (2001), Watershed control on the carbon loading of marine sedimentary particles, *Geochim. Cosmochim. Acta*, *65*, 2231–2240.

Martin, D. P., C. A. Nittrouer, A. S. Ogston, and J. S. Crockett (2007), Tidal and seasonal dynamics of a muddy inner shelf environment, Gulf of Papua, *J. Geophys. Res.*, doi:10.1029/2006JF000681, in press.

Mayer, L. M. (1994), Surface area control of organic carbon accumulation in continental shelf sediments, *Geochim. Cosmochim. Acta*, *58*, 1–14.

Mayer, L. M., R. G. Keil, S. A. Macko, S. B. Joye, K. C. Ruttenberg, and R. C. Aller (1998), Importance of suspended particulates in riverine delivery of bioavailable nitrogen to coastal zones, *Global Biogeochem. Cycles*, *12*, 573–579.

McAlpine, J. R., and G. Keig (1983), *Climate of Papua New Guinea*, 200 pp., Aust. Natl. Univ. Press, Canberra.

McKinnon, A. D., J. H. Carleton, and S. Duggan (2007), Pelagic production and respiration in the Gulf of Papua during May 2004, *Cont. Shelf Res.*, *27*, 1643–1655.

Milliman, J. D., and J. P. M. Syvitski (1992), Geomorphic/tectonic control of sediment discharge to the ocean: The importance of small mountainous rivers, *J. Geol.*, *100*, 525–544.

Nittrouer, C. A., and S. A. Kuehl (1995), Geological significance of sediment transport and accumulation on the Amazon continental shelf, *Mar. Geol.*, *125*, 175–176.

Nittrouer, C. A., and R. W. Sternberg (1981), The formation of sedimentary strata in an allochthonous shelf environment: The Washington continental shelf, *Mar. Geol.*, *42*, 201–232.

Nittrouer, C. A., S. A. Kuehl, D. J. DeMaster, and R. O. Kowsmann (1986), The deltaic nature of Amazon shelf sedimentation, *Geol. Soc. Am. Bull.*, *97*, 444–458.

Ogston, A. S., R. W. Sternberg, C. A. Nittrouer, D. P. Martin, M. A. Goñi, and J. S. Crockett (2007), Sediment delivery from the Fly River tidally dominated delta to the nearshore marine environment and the impact of El Niño, *J. Geophys. Res.*, doi:10.1029/2006JF000669, in press.

Opsahl, S., and R. Benner (1995), Early diagenesis of vascular plant tissues: Lignin and cutin decomposition and biogeochemical implications, *Geochim. Cosmochim. Acta*, *59*, 4889–4904.

Prahl, F. G., J. R. Ertel, M. A. Goni, M. A. Sparrow, and B. Eversmeyer (1994), Terrestrial organic carbon contributions to sediments on the Washington margin, *Geochim. Cosmochim. Acta*, *58*, 3035–3048.

Quideau, S. A., R. C. Graham, X. Feng, and O. A. Chadwick (2003), Natural isotopic distribution in soil surface horizons differentiated by vegetation, *Soil Sci. Soc. Am. J.*, *67*, 1544–1550.

Robertson, A. I., and D. M. Alongi (1995), Role of riverine mangrove forests in organic carbon export to the tropical coastal ocean: A preliminary mass balance for the Fly delta (Papua New Guinea), *Geo Mar. Lett.*, *15*, 134–139.

Robertson, A. I., P. A. Daniel, P. Dixon, and D. M. Alongi (1993), Pelagic biological processes along a salinity gradient in the Fly delta and adjacent river plume (Papua New Guinea), *Cont. Shelf Res.*, *13*, 205–224.

Robertson, A. I., P. Dixon, and D. M. Alongi (1998), The influence of fluvial discharge on pelagic production in the Gulf of Papua, Northern Coral Sea, *Estuarine, Coastal Shelf Sci.*, *46*, 319–331.

Stuiver, M., and H. A. Polach (1977), Discussion: Reporting of ^{14}C data, *Radiocarbon*, *19*, 355–363.

Taylor, J. R. (1997), *An Introduction to Error Analysis*, 327 pp., Univ. Sci., Sausalito, Calif.

Thom, B. G., and L. D. Wright (1983), Geomorphology of the Purari delta, in *The Purari: Tropical Environment of a High Rainfall River Basin*, edited by T. Petr, 624 pp., Springer, New York.

Vail, P. R., R. M. Mitchum Jr., R. G. Todd, J. M. Widmier, S. Thompson III, J. B. Sangree, J. N. Bubb, and W. G. Hatlelid (1977), Seismic stratigraphy and global changes of sea level, in *Seismic Stratigraphy—Applications to Hydrocarbon Exploration*, edited by C. E. Payton, *Am. Assoc. Pet. Geol. Mem.*, *29*, 49–211.

Vogel, J. J., J. R. Southen, and D. E. Nelson (1987), Catalyst and binder effects in the use of filamentous graphite for AMS, *Nucl. Instrum. Methods Res., Sect. B*, *29*, 50–56.

Walsh, J. P., and C. A. Nittrouer (2003), Contrasting styles of off-shelf sediment accumulation in New Guinea, *Mar. Geol.*, *196*, 105–125.

Walsh, J. P., C. A. Nittrouer, C. M. Palinkas, A. S. Ogston, R. W. Sternberg, and G. J. Brunskill (2004), Clinoform mechanics in the Gulf of Papua, *Cont. Shelf Res.*, *24*, 2487–2510.

Wolanski, E., B. King, and D. Galloway (1995), Dynamics of the turbidity maximum in the Fly River Estuary, Papua New Guinea, *Estuarine Coastal Shelf Sci.*, *40*, 321–337.

Wolanski, E., B. King, and D. Galloway (1997), Salinity intrusion in the Fly River estuary, Papua New Guinea, *J. Coastal Res.*, *13*, 983–994.

R. Aalto, Department of Earth and Space Sciences, University of Washington, Seattle, WA 98195, USA.

S. R. Alin, J. Crockett, C. Nittrouer, and A. Ogston, School of Oceanography, University of Washington, Seattle, WA 98195, USA.

R. Gisewhite, Department of Marine Sciences, University of Georgia, Athens, GA 30602-3636, USA.

M. A. Goni, College of Oceanic and Atmospheric Sciences, Oregon State University, Corvallis, OR 97331, USA. (mgoni@coas.oregonstate.edu)

N. Monacci, School of Fisheries and Ocean Sciences, University of Alaska Fairbanks, Fairbanks, AK 99775, USA.